CHAPTER 6

RHEOLOGY AND PERFORMANCE EVALUATION OF BITUMINOUS MASTICS

6.1 Preamble

This chapter investigated the effect of fillers on the rheology and performance of bituminous mastics against rutting, fatigue, and ageing. The bituminous mastics were prepared as per the filler bitumen ratios determined in Chapter 4. The physical properties of mastics were investigated using a softening point test. Since bitumen is viscoelastic material at service temperatures, the rheological behavior of bitumen and mastics were investigated at different testing temperatures and loading frequencies by performing dynamic mechanical analysis using a Dynamic Shear Rheometer (DSR). The rutting resistance at high temperatures and fatigue resistance of mastics at intermediate temperature were investigated using standard rutting and fatigue parameters defined in Superpave specification. However, the reliability of the Superpave parameters in analyzing the performance of mastics is quite questionable, according to several previous studies. Hence, the performance of mastics in terms of rutting and fatigue was also investigated using Multiple Stress Creep and Recovery (MSCR) and Linear Amplitude Sweep (LAS) analysis, respectively. In addition to above mentioned methods, this section also investigated the potential of a relatively new approach based on the MSCR test to assess the fatigue resistance of bitumen and mastics. Finally, the influence of waste and conventional fillers on long-term ageing resistance of mastics was also analyzed. It was done by calculating the ageing index of mastics by comparing the values of complex shear modulus of long-term and

short-term aged mastics. A minimum of three specimens was tested for each test, and the average values of the obtained results are reported.

Plate 6.1 Preparation of bituminous mastic using mechanical mixer

6.2 Preparation of Bituminous Mastics

There is no well-defined procedure specified in Indian specification for the preparation of bituminous mastics. All mastics were prepared using a common procedure to minimize the variability amongst results. First, 500 g of fillers were preheated overnight in an oven maintained at 135°C. Then, 500 g of bitumen was also separately heated in another oven at the same temperature for an hour to maintain sufficient fluidity. The mass of bitumen needed to make mastic at the required filler bitumen ratio with 100 g of filler is determined and weighed. The weighed filler was divided into five equal portions. Each portion was mixed with bitumen using a mechanical mixer having 1600 rpm speed maintained at 160 ±5°C for 10 minutes (Plate 6.1). After the addition of all five portions, the mixing is continuously done for half an hour to ensure the uniform mixing of mastic. The filler bitumen ratio for mastics was decided according to the filler content and OBC of the mix, as determined in Chapter 5. The selected filler bitumen ratio for the mastics is mentioned

in Table 6.1, which is adopted in the entire study. The filler volume fraction of filler for mastics was determined using Equation 6.1 given below.

$$V_f = \frac{\frac{M_f}{G_f}}{\frac{M_f}{G_f} + \frac{M_b}{G_b}} \quad [6.1]$$

Where: V_f = Filler volume fraction

M_f = Mass of filler in mastic

G_f = Specific gravity of filler in mastic

M_b = Mass of bitumen in mastic

G_b = Specific gravity of bitumen in mastic

Table 6.1 Various properties of mastics

Type of filler	Filler content in the bituminous mix (%)	Abbreviation of mastic	Effective filler bitumen ratio of mastic (by mass)	Filler volume fraction
Stone dust	4.0	SD 4	0.66	0.1964
	5.5	SD 5.5	0.96	0.2623
	7.0	SD 7	1.38	0.3398
	8.5	SD 8.5	1.76	0.3891
Kota stone	4.0	KS 4	0.70	0.2088
	5.5	KS 5.5	1.06	0.2855
	7.0	KS 7	1.45	0.3536
	8.5	KS 8.5	1.82	0.4220
Glass powder	4.0	GP 4	0.71	0.2304
	5.5	GP 5.5	1.04	0.3048
	7.0	GP 7	1.46	0.3826
	8.5	GP 8.5	1.87	0.4486
Glass-hydrated lime	4.0	GL 4	0.77	0.2453
	5.5	GL 5.5	1.15	0.3267
	7.0	GL 7	1.60	0.4030
	8.5	GL 8.5	2.00	0.4588

6.3 Ageing of Bituminous Mastics

6.3.1 Short-Term Ageing

To simulate the construction hardening, the short-term ageing of the bitumen and mastics was done. It must be noted that there is an absence of a well-defined

protocol for the ageing of the bituminous mastic, and usually, the methods used to simulate the ageing in bitumen also applied for the mastics. In this study, the short-term ageing of bitumen and mastics was done using thin film oven procedure as stated in ASTM D1754-94 (1995a) protocol (Plate 6.2). As per the procedure, the hot mastic/bitumen is placed in the rotating shelves (5.5±1 rpm) of the oven maintained at 163°C for 5 h. The residue obtained after the ageing is used for testing and analysis.

Plate 6.2 Thin film oven used in this study

Plate 6.3 Moisture oven used in this study

6.3.2 Long-Term Ageing

Long-term ageing test simulates the gradual hardening of bitumen and mastic due to their environmental exposure over their service life. This test is usually performed using the pressure ageing vessel. Due to the unavailability of this apparatus in the parent institute, an alternative protocol suggested in a recent Indian study was followed to simulate long-term ageing (Behara et al., 2013). It utilized the normal moisture oven to simulate the long-term ageing equivalent to that of pressure ageing vessel (Plate 6.3). As per this protocol, a given weight of short-term aged bitumen and

mastic was calculated so that they can form a film thickness of 650μm on the circular pan having diameter 140 mm. These pans were placed into a regular oven maintained at 85°C for 5 days. The residue remaining after the ageing was used in further testing and analysis.

Plate 6.4 (a) Determination of softening point in water

Plate 6.4 (b) Determination of softening point in glycerine

6.4 Softening Point of Bituminous Mastics

The ring and ball softening point test is an empirical method used to measure the consistency of bituminous mastic and to analyze the stiffening effect of fillers. The softening point test of short-term aged mastics was conducted similar to that of bitumen as per the IS 1205 (1978) protocol. The test procedure are already specified in detail in Section 4.3.2.3. The mastics, which were expected to have softening points lower than 80°C were tested in water, while the mastics with softening points higher than 80°C were tested in glycerine. The test setup is shown in Plate 6.4.

The softening point of short-term aged bitumen was determined to be 54°C. The softening point of the mastics found to increase with the filler content or with the filler bitumen ratio (Table 6.2). It was attributed to the stiffening effect of the fillers due to their increase in filler volume fraction in mastic with the filler content (Table

6.1). The GL mastics had the highest softening point values at each filler concentration, followed by GP, KS, and SD mastics. It was quite evident since both hydrated lime and glass powder have the lowest specific gravities as well as higher void contents due to which they occupy higher volume in mastic and also resulted in lower amount of free bitumen in the mastic. The conventional SD mastics have lowest softening point amongst all mastics.

Table 6.2 Softening point of various mastics

Type of mastic	Softening point (°C)
SD 4	55.92
SD 5.5	61.50
SD 7	66.25
SD 8.5	69.50
GP 4	60.50
GP 5.5	67.25
GP 7	75.17
GP 8.5	85.50
KS 4	60.17
KS 5.5	64.50
KS 7	69.42
KS 8.5	74.25
GL 4	63.25
GL 5.5	70.17
GL 7	80.50
GL 8.5	92.25

6.5 Testing of Bituminous Mastics with Dynamic Shear Rheometer

6.5.1 Purpose, Principle and Instrumentation

Bitumen is a viscoelastic material, possessing both elastic and viscous characteristics, which depends on both loading time and testing temperatures. Hence, an empirical method such as softening point is unable to accurately predict the performance of bitumen, mastic, and subsequently the bituminous mixes for over a wide range of loading time and temperature. Dynamic mechanical analysis is conducted in this study with dynamic shear rheometer to determine the elastic and viscous nature of bitumen and mastics over a wide range of temperatures and loading frequencies. To conduct

dynamic mechanical analysis, a thin bitumen/mastic specimen is placed in between two parallel plates, as shown in Figure 6.1.

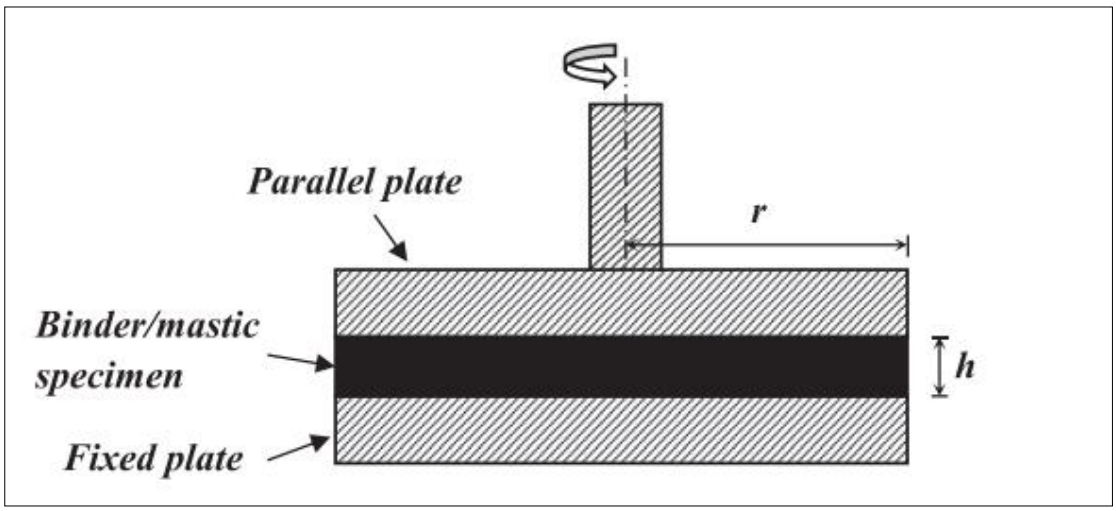

Figure 6.1 Line diagram of dynamic shear rheometer

Plate 6.5 Dynamic shear rheometer used in this study (Anton Paar MCR 101)

This specimen is subjected to a shear stress or strain of a constant or varying magnitude in different modes such as oscillatory (sinusoidally varying stress or strain), viscometry (monotonic shear), or creep and recovery. However, strain control testing in oscillatory mode is usually more preferred in which sinusoidal varying

stress is applied, and response in terms of strain is measured (Saboo, 2015; Yusoff, 2012). In the oscillatory mode of testing, the bottom plate remains stationary, while the top plate (movable spindle) oscillates at the chosen angular frequency. This in turn helps to measure the rheological properties of bitumen and mastics at different temperatures, frequencies, and at different magnitudes of stress and strain. This study utilized Anton Paar's MCR 101 DSR which is shown in Plate 6.5. Its operation, temperature control, data acquisition, and analysis are done with the help of computer attached to it. DSR applies a sinusoidal strain as an oscillatory shear on the bitumen/mastic sample, and measures the amplitude of responding stress by determining the torque transmitted through it. The stress and strain parameters can be calculated according to Equations 6.2 and 6.3

$$\tau = \frac{2T}{\pi r^3} \quad [6.2]$$

Where: τ = Shear stress

T = Torgue

r = Radius of the spindle/test sample

$$\gamma = \frac{\theta r}{h} \quad [6.3]$$

Where: γ = Shear Strain

θ = Deflection angle

r = Radius of the spindle/test sample

h = Gap between the parallel plates

The diameter of the spindle and gap between the plates depends upon the testing temperatures. Usually testing at higher temperatures (46°C or higher) requires arrangement having a spindle with 25 mm diameter with 1 mm gap, while testing at intermediate and lower temperatures (4-46°C) needed 8 mm diameter spindle and 2

mm gap. This is done to apply torque in such a way so it falls within the loading capabilities of DSR.

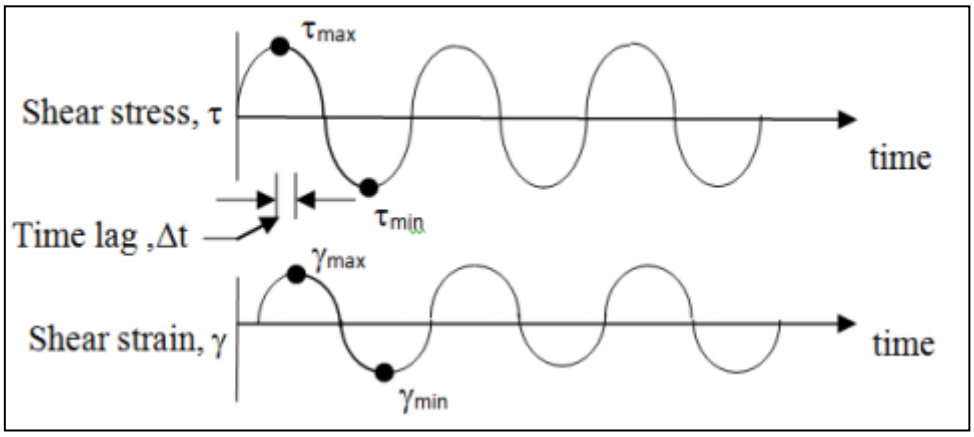

Figure 6.2 Variation of stress and strain with time in a DSR test

For each combination of temperature and frequency, DSR measures two primary parameters known as complex shear modulus (G*) and phase angle (δ). Complex shear modulus measures the resistance of a material against shear when it is subjected to the repeated shear. It is the ratio of maximum shear stress (τ_{max}) to the maximum shear strain (γ_{max}). Phase angle computes the relative magnitude of elastic (recoverable) and viscous (non-recoverable) deformations. It is the product of the angular frequency (ω) of the loading and the time lag (Δt) between the stress and strain. A typical stress strain plot produced in DSR analysis is shown in Figure 6.2. The perfectly elastic material has zero phase angle as it shows instant response to applied stress, while perfectly viscous liquid has large time lag and its phase angle approaches to 90º. Since bitumen and mastics are viscoelastic materials, their phase angles fall within the two extremes at pavement service temperatures.

6.5.2 Sample Preparation

In this study, the hot pour method is used to prepare sample for testing. The hot pour method is based on the Methods 1 and 3 of the SHRP A 370 protocol, Alternative 1 of

the AASHTO TP5 and AASHTO T315 standards (AASHTO, 1998; AASHTO, 2020; Celauro et al., 2012; Petersen et al., 1994). As per this method, the gap between the spindle and plate has been set as per the test requirement plus 50 µm. After setting the required gap, the sufficient quantity of fluidic sample (bitumen or mastic) is poured on to the bottom plate. The spindle is then lowered to the required testing gap plus 50 µm and the excess bitumen which squeezed out of the edges should be carefully trimmed off with the help of a trimming tool. After trimming, the remaining 50 µm gap has also been closed and the sample was set to the required testing temperature.

6.5.3 Determination of High Temperature Performance Grade of Bitumen

The objective of this study is to investigate the rheological properties of bitumen at intermediate and high temperatures. In order to finalize the testing temperatures of the bitumen and mastics, it is necessary to determine the highest temperature up to which the bitumen displays satisfactory performance in term of rutting resistance. This can be done by determining the upper PG temperature of bitumen after testing the un-aged and short-term aged bitumen as per AASHTO T320 protocol. The test was performed in controlled strain mode, over a temperature range of 46 to 76°C with gradual increment of 6°C. Sinusoidal strain of 12% (for un-aged) and 10% (for short-term aged) sample was applied at varying temperatures with frequency of 10 rad/s. DSR automatically controls the strain without any assistance by the operator. The maximum temperatures at which the un-aged bitumen and short-term aged bitumen displayed minimum $G^*/\sin\delta$ of 1.0 kPa and 2.2 kPa, respectively were identified. The 70°C was observed as smaller of the both temperatures and it was identified as the upper PG temperature. Hence the temperature range for the analysis of rheological properties of bitumen and mastics at high temperature is finalized as 46-70°C.

6.5.4 Determination of Linear Viscoelastic Limits using Strain Sweep Test

Bitumen and bituminous mastics are viscoelastic materials, however, their viscoelastic response can be divided into two behavioural domains as linear viscoelastic and non-linear viscoelastic. Any material behaves as linear viscoelastic material when its viscoelastic properties (such as complex modulus and creep compliance) are dependent on temperature and frequency of loading but independent of the magnitude of stress (Airey, 1997; Saboo, 2015). The assumption of bitumen being a linear viscoelastic material makes the analysis easier and convenient as compared to nonlinear analysis. Also the interdependency of the loading frequency and temperatures (time-temperature superposition) are only valid in linear viscoelastic region. Usually bitumen and mastics doesn't display non-linear behaviour at the strain amplitude lower than a certain limit (depending upon the type of material, temperature, and frequency), which can be defined as its linear viscoelastic limit (LVE). Hence it is necessary to determine this strain amplitude and limit the rheological characterization of materials below this LVE limit.

The strain sweep test was conducted on bitumen and mastics to determine their LVE limits. This test was conducted at intermediate (25ºC) and high (46-70ºC with 6ºC increments) temperatures at a frequency of 10 rad/s or 1.59 Hz. This frequency is chosen since it can simulate the stress wave similar to the movement of vehicle at the speed of 50-60 mph (80-96 kmph) on the surface layer at the field. The spindle of 8 mm diameter with 2 mm plate gap was used for testing at intermediate temperature, while spindle having 25 mm diameter with 1 mm gap was used in higher temperatures. During the test, the magnitude of strain was varied for 0-100% to ensure the sweep was done in both linear and non-linear domain. Previous studies

identified LVE limits as the strain level at which the complex modulus of the material decreased to 95 percent of its initial value.

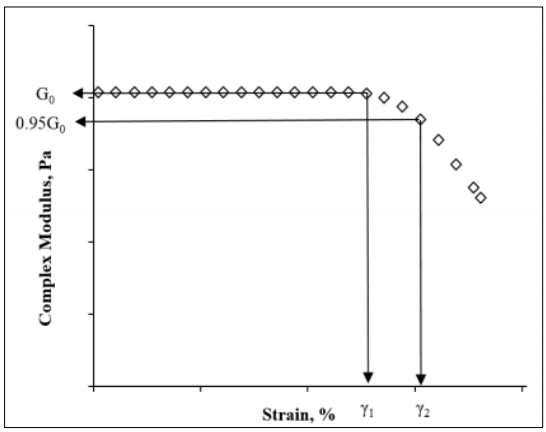

Figure 6.3 Schematic representation of strain sweep test (Saboo, 2015)

This could be schematically represented as the typical curve presented in Figure 6.3. In this figure, G_0 is the initial linear viscoelastic modulus, γ_1 is the strain at which the initial modulus starting to get decrease and it can be identified as the point for the onset of non-linear behaviour. γ_2 represents the strain equivalent to 95% of the initial modulus. According to specification, the viscoelastic region which falls below this strain level is linear viscoelastic region for the bitumen and mastics, and this strain or any strain below than this can be utilized in frequency sweep and other testing.

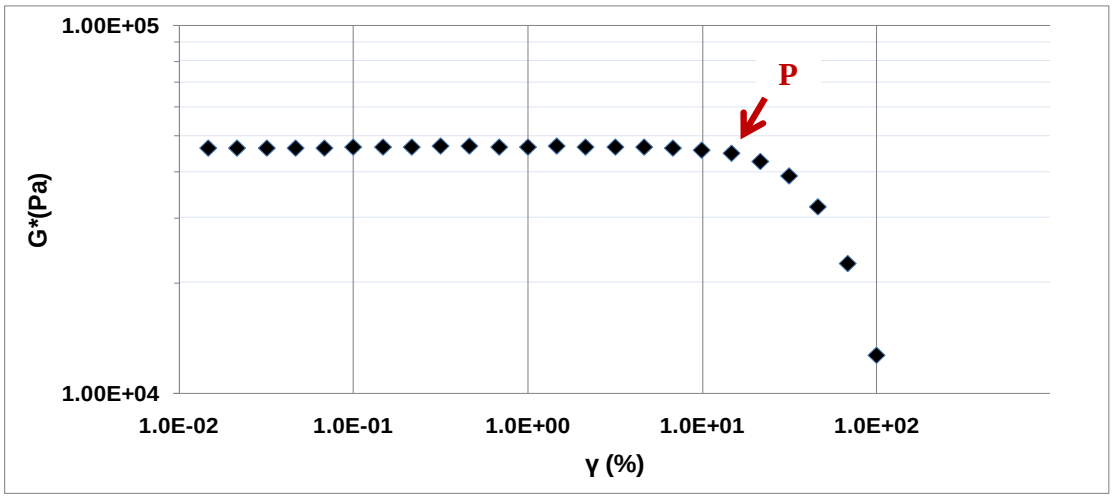

Figure 6.4 Variation of stress and strain in strain sweep test of bitumen at 46ºC

Figure 6.4 displayed an example for analysis of LVE range of the bitumen at 46ºC. Here, the strain corresponds to identified point "P" (14.7%) is termed as LVE limit

strain and any lower strain can be employed for the testing performed in LVE region. Table 6.3 presents LVE strain limits of different mastics which are also shown in Figure 6.5. It can be clearly observed that LVE strain for bitumen and mastics increases with increase in temperature. The bitumen and mastics display lower stiffness at higher temperatures and hence they needed higher strain levels to reach to non-linear viscoelastic region. All mastics have LVE range lower than the plain bitumen, which can be attributed to their relatively higher stiffness. Mastics also found to have lower temperature susceptibility than plain bitumen as they have lower rate of LVE increase with the temperature. Also, LVE values of mastic decreases with the increase in filler content due to increase in the stiffness of the mastics caused due to solid inert filler particles in the mastics. In general, GL mastics have the lowest LVE values followed by GP, KS, and SD mastics. It was evident since mastics having lower bitumen content and higher filler volume fraction display higher stiffening.

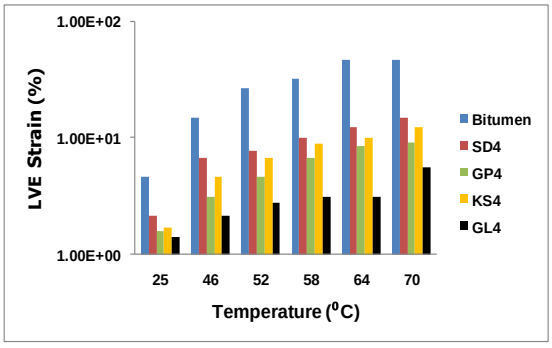

(a) Mastics corresponds to mixes with 4% filler

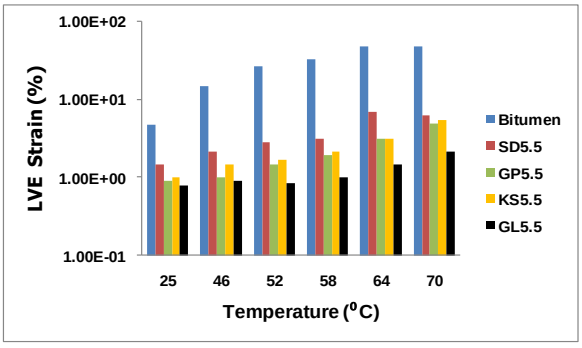

(b) Mastics corresponds to mixes with 5.5% filler

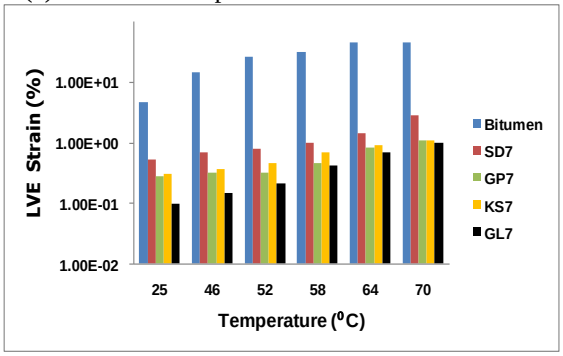

(c) Mastics corresponds to mixes with 7% filler

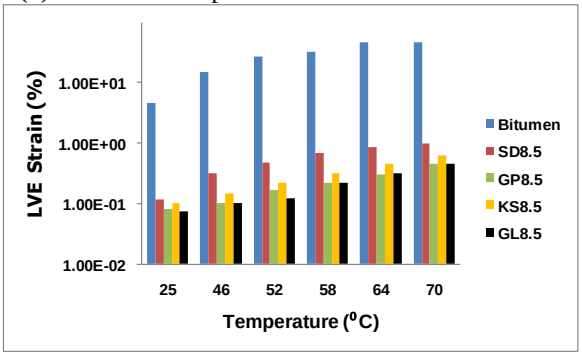

(d) Mastics corresponds to mixes with 8.5% filler

Figure 6.5 LVE strain (%) limits for various mastics

Table 6.3 LVE strains of different mastics

Type of mastic	LVE strain limit (%) at different temperatures					
	25ºC	46ºC	52ºC	58ºC	64ºC	70ºC
Bitumen	4.65E+0	1.47E+1	2.66E+1	3.17E+1	4.64E+1	4.64E+1
SD 4	2.15E+0	6.73E+0	7.80E+0	1.00E+1	1.24E+1	1.47E+1
SD 5.5	1.47E+0	2.15E+0	2.82E+0	3.16E+0	6.81E+0	6.81E+0
SD 7	5.20E-1	6.81E-1	7.87E-1	1.00E+0	1.47E+0	2.81E+0
SD 8.5	1.16E-1	3.16E-1	4.64E-1	6.81E-1	8.41E-1	1.00E+0
GP 4	1.61E+0	3.16E+0	4.64E+0	6.81E+0	8.41E+0	9.12E+0
GP 5.5	9.12E-1	1.00E+0	1.47E+0	1.92E+0	3.16E+0	4.80E+0
GP 7	2.81E-1	3.16E-1	3.16E-1	4.64E-1	8.41E-1	1.10E+0
GP 8.5	8.00E-2	1.00E-1	1.70E-1	2.15E-1	3.00E-1	4.60E-1
KS 4	1.70E+0	4.64E+0	6.81E+0	8.93E+0	10.00E+0	12.35E+0
KS 5.5	1.00E+0	1.47E+0	1.70E+0	2.15E+0	3.16E+0	5.40E+0
KS 7	3.00E-1	3.65E-1	4.64E-1	6.81E-1	9.00E-1	1.10E+0
KS 8.5	1.00E-1	1.47E-1	2.15E-1	3.16E-1	4.60E-1	6.10E-1
GL 4	1.41E+0	2.16E+0	2.80E+0	3.16E+0	3.16E+0	5.60E+0
GL 5.5	7.87E-1	8.93E-1	8.41E-1	1.00E+0	1.47E+0	2.16E+0
GL 7	1.00E-1	1.47E-1	2.15E-1	4.15E-1	7.00E-1	1.00E+0
GL 8.5	7.32E-2	9.94E-2	1.22E-1	2.15E-1	3.16E-1	4.60E-1

6.5.5 Rheological Analysis using Frequency Sweep Test

The rheological properties of short-term aged bitumen and mastics were determined using frequency sweep conducted at intermediate (25ºC) and high temperatures (46-70 ºC). The testing is done at the strains below than the LVE limits of mastics. The testing is conducted in a frequency range of 0.1-100 rad/s to analyze the effect of traffic speed on rheological properties. As stated before, the arrangement of 8 mm diameter spindle with 2 mm plate gap was used for testing at intermediate temperature, while 25 mm diameter spindle with 1 mm gap was used in high temperature testing. The complex shear modulus (G*) and phase angle (δ) of bitumen and mastics were determined at different combinations of temperatures and frequencies. The isothermal plots and black diagrams were plotted to analyze the variation amongst the rheological properties. Isothermal plots are used to compare different viscoelastic functions (such as complex shear modulus and phase angle) at different frequencies and at same temperature.

The isothermal plots of complex shear modulus and phase angle are shown in Figure 6.6 to 6.14. In general, it was observed that inclusion of filler content in the mastic tends to increase the complex modulus and decrease in the phase angle of the mastic. The greater the complex modulus, higher is the stiffness of mastic. While smaller the value of phase angle, higher is the elasticity of the mastic. The increase in complex modulus and decrease in phase angle was observed with the increase in filler content at each loading frequency. This increase in complex modulus of mastic with the filler content was found to follow similar trend as the softening points determined in previous section. The stiffness of bitumen and mastics were found to increase with the decrease in temperature and increase in frequency.

The increase in complex modulus with the frequency (in terms of slope of curve) was calculated and stated in Table 6.4. It was observed that for any mastic, increase in complex modulus with frequency increases with the testing temperature. Hence, it can be said that the mastics becomes more susceptible to speed of traffic loading at a higher temperature. It was also observed that at the same temperature, mastics with higher stiffness displayed lower rate of growth in complex modulus. Hence it can be inferred that the stiffer mastics are less susceptible to the rate of traffic loading and vice versa. The rate of change of phase angle with the frequency (in terms of slope of curve) is displayed in Table 6.5. The rate of decrease in phase angle was found to decrease with increase in the temperature. However rate of decrease in phase angle doesn't found to have any proper trend with the stiffness of mastic.

The viscoelastic properties of mastics were also compared at the frequency of 10 rad/s at high temperatures which are displayed in Figures 6.15 and 6.16. The mastics prepared with GL displayed highest complex modulus followed by GP, KS, and SD.

Also, GL mastic displayed lowest phase angle followed by GP, KS, and SD. The higher complex modulus in GL and GP mastics might be due to the reinforcement provided by filler particles due to their relatively higher volume concentration in these mastics (Buttlar et al., 1999; Zhang et al., 2013). Apart from the volumetric reinforcement, the higher complex modulus of GP and GL mastic might also be due to the angular nature of GP which resulted in better interlocking amongst particles (Cosme et al., 2016). The rate of increase in stiffness of mastic is also influenced by the filler volume concentration. From the Figure 6.15, it is clearly observed that rate of increase of complex modulus is low in case of 4 and 5.5% filler mastics. However, the complex modulus was found to increase at higher rate in case of higher filler concentration. Previous studies (Bautista, 2015; Faheem and Bahia, 2010; Liao et al., 2012) have theorized that stiffness in the mastic increases linearly up to a critical filler volume concentration. The further addition of the filler led to non linear and rapid rate of increase in complex modulus. The region up to which the complex modulus increases linearly is known as diluted region, while the region displaying non linear rapid growth in complex modulus is known as concentrated region. All mastics displayed steady growth in complex modulus up to 5.5% filler concentration and then observed a relatively rapid growth (higher slope) at higher concentration (7 and 8.5%) (Figure 6.15). The rapid increase in the stiffening for mastics might be attributed to the fillers contributing such a large volume to the mastics that they become a predominant component in it. At this concentration, the filler particles gets close enough to each other and cause interaction which exhibits a dramatic increase in the complex modulus (Liao et al., 2012; Zhang et al., 2017). GL and GP mastics especially experienced higher increase in complex modulus in this region which might be due to the lower volume of free bitumen and higher filler volume

concentration in these mastics. GL and GP mastics also observed higher drop in phase angles in this region especially at higher temperatures in comparison to SD and KS mastics (Figure 6.16).

Black diagram is the plot of complex modulus versus the phase angle which is used to analyze the effect of ageing and the modification in bitumen and mastics. Black diagrams of various mastics were plotted in Figures 6.17. It was observed that increase in filler concentration tends to shift black curve to upwards and left direction. This signified the increase in the complex modulus and decrease in phase angle with the increase in filler concentration in the mastic. The black curves of pure bitumen, SD, and KS mastics are found to be smooth which signified a consistent relationship between complex modulus and phase angle of these mastics throughout the frequencies and temperature. This trend is expected since the analysis is performed in the linear viscoelastic region when interdependency of the loading frequency and temperatures (time-temperature superposition) exists. However black diagrams of GL and GP mastics don't exhibit simple smooth curves at higher filler concentration, especially at higher temperature and lower frequency. This confirmed the dominance of filler volume concentration on viscoelastic behaviour of GL and GP mastics.

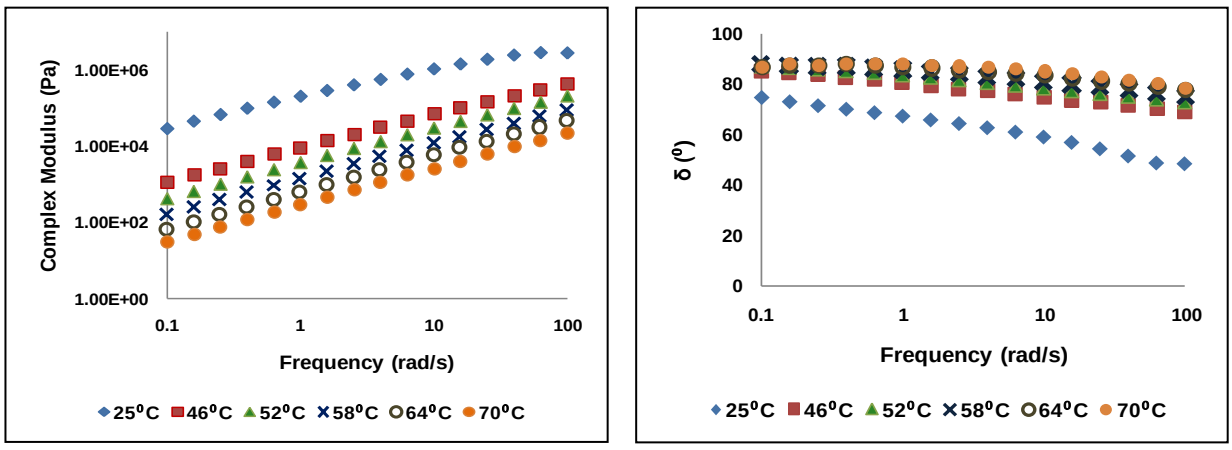

(a) Isothermal curves of the complex shear modulus of bitumen

(b) Isothermal curves of the phase angle of bitumen

Figure 6.6 Isothermal curves of bitumen

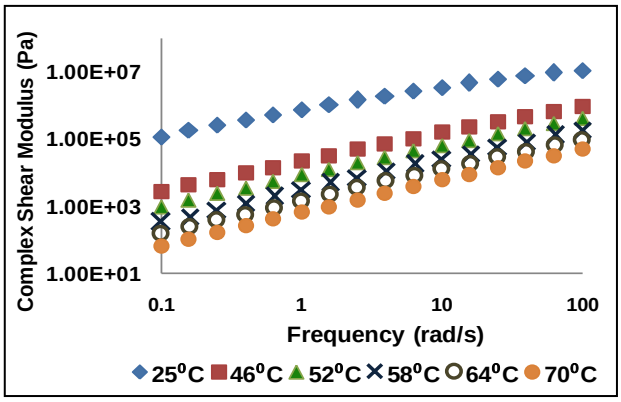

(a) Complex shear modulus of SD4 mastics

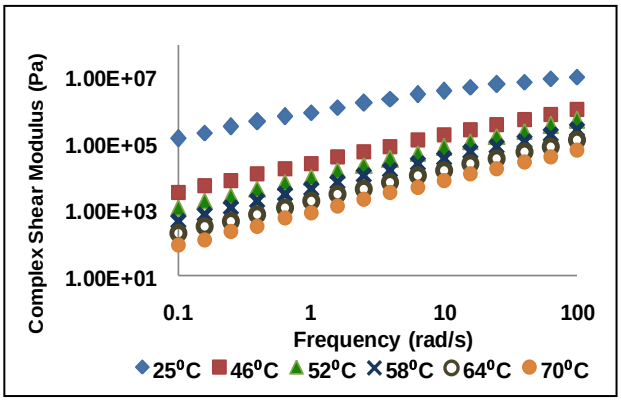

(b) Complex shear modulus of KS4 mastics

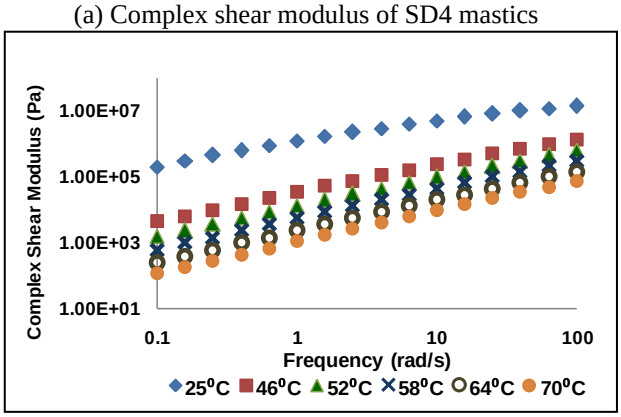

(c) Complex shear modulus of GP4 mastics

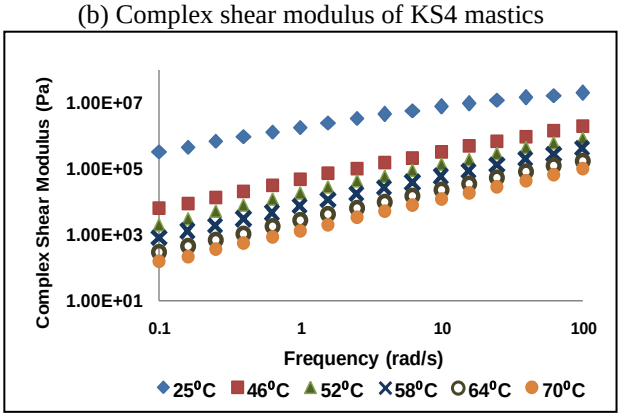

(d) Complex shear modulus of GL4 mastics

Figure 6.7 Isothermal curves of the complex shear modulus of mastics corresponding to 4% filler

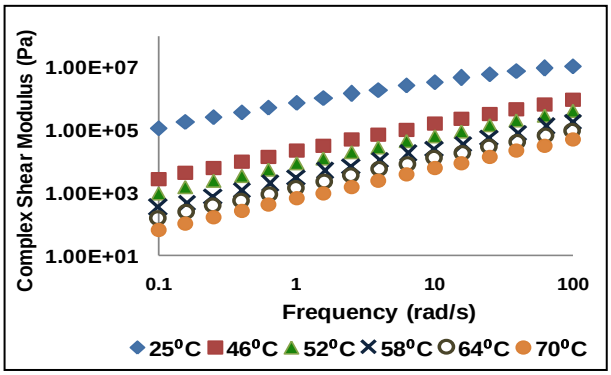

(a) Complex shear modulus of SD 5.5 mastics

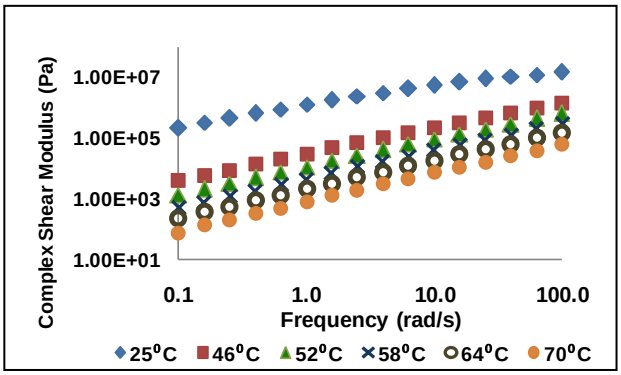

(b) Complex shear modulus of KS 5.5 mastics

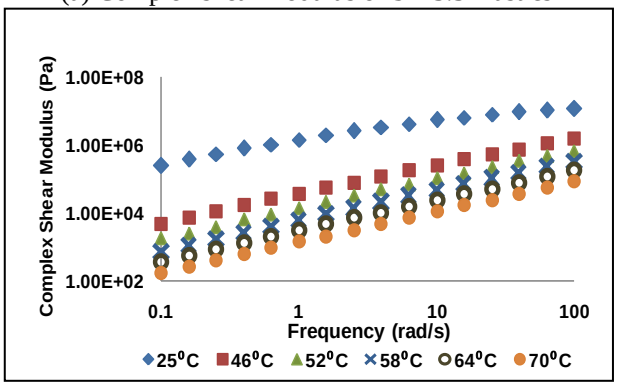

(c) Complex shear modulus of GP 5.5 mastics

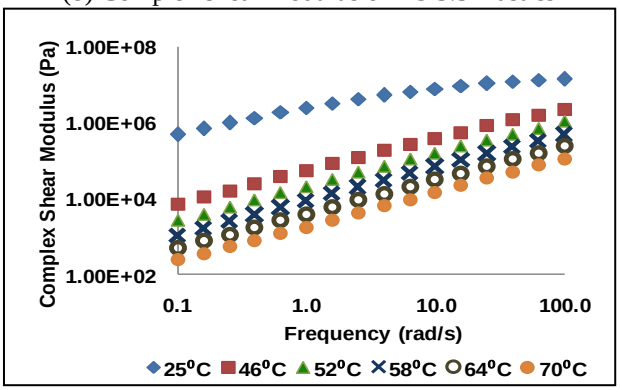

(d) Complex shear modulus of GL 5.5 mastics

Figure 6.8 Isothermal curves of complex shear modulus of mastics corresponding to 5.5% filler

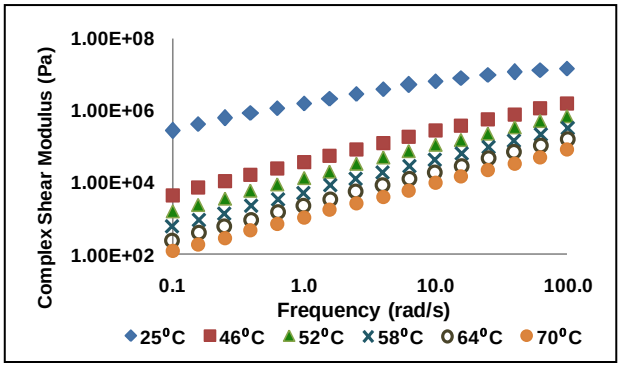

(a) Complex shear modulus of SD 7 mastics

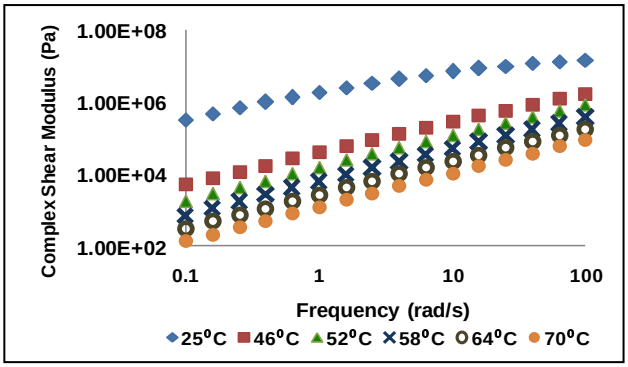

(b) Complex shear modulus of KS 7 mastics

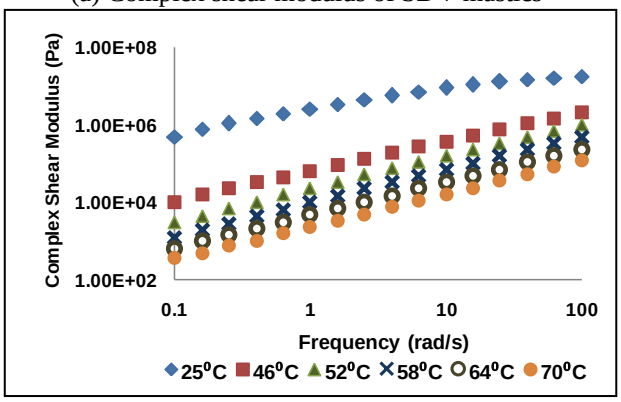

(c) Complex shear modulus of GP 7 mastics

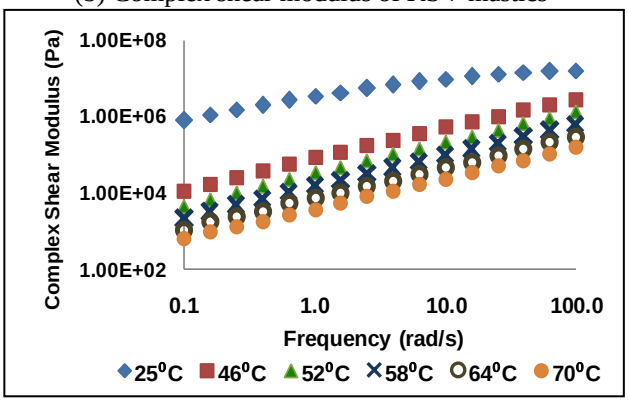

(d) Complex shear modulus of GL 7 mastics

Figure 6.9 Isothermal curves of the complex shear modulus of mastics corresponding to 7% filler

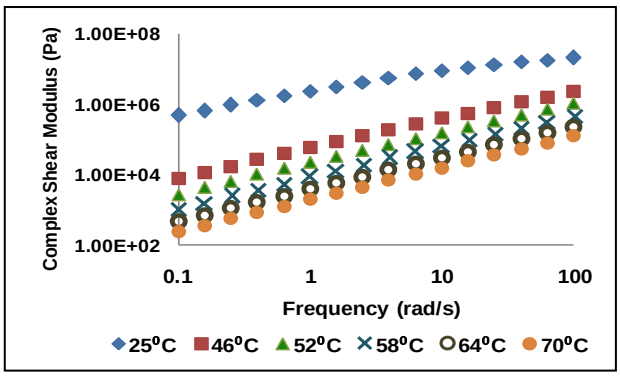

(a) Complex shear modulus of SD 8.5 mastics

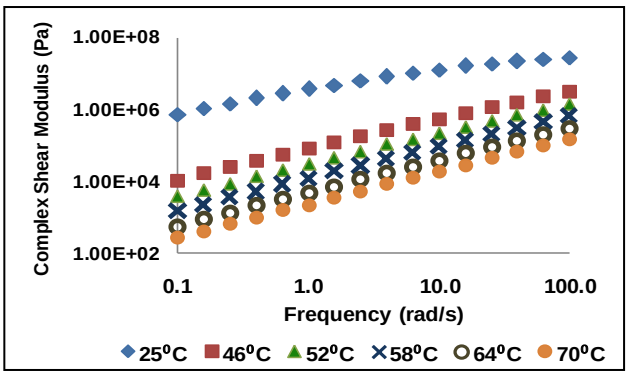

(b) Complex shear modulus of KS 8.5 mastics

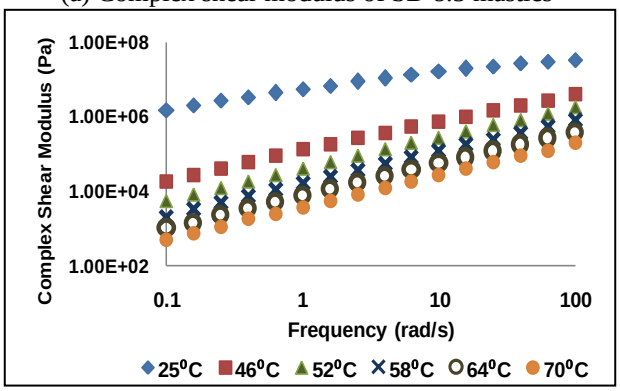

(c) Complex shear modulus of GP 8.5 mastics

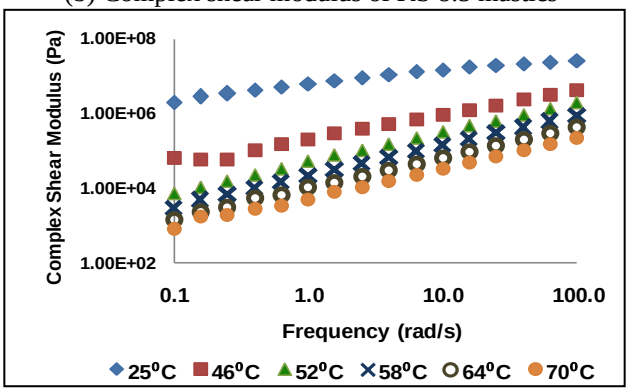

(d) Complex shear modulus of GL 8.5 mastics

Figure 6.10 Isothermal curves of complex shear modulus of mastics corresponding to 8.5% filler

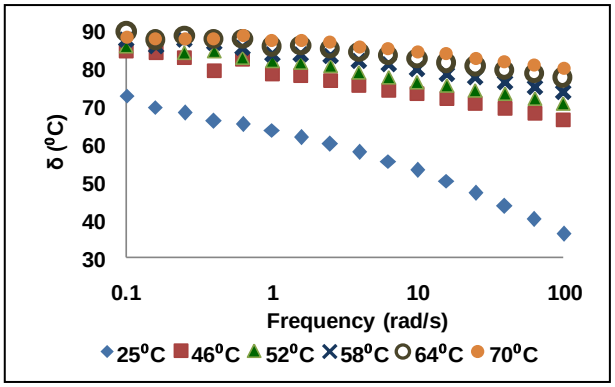

(a) Isothermal curves of the phase angle of SD 4 mastics

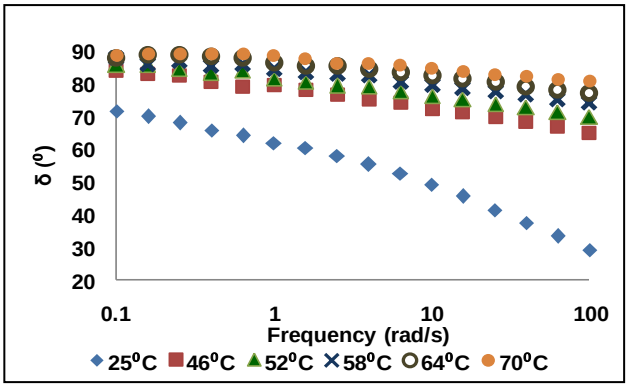

(b) Isothermal curves of the phase angle of KS 4 mastics

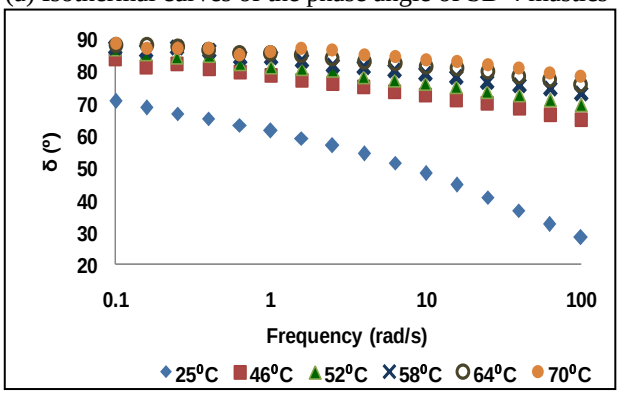

(c) Isothermal curves of the phase angle of GP 4 mastics

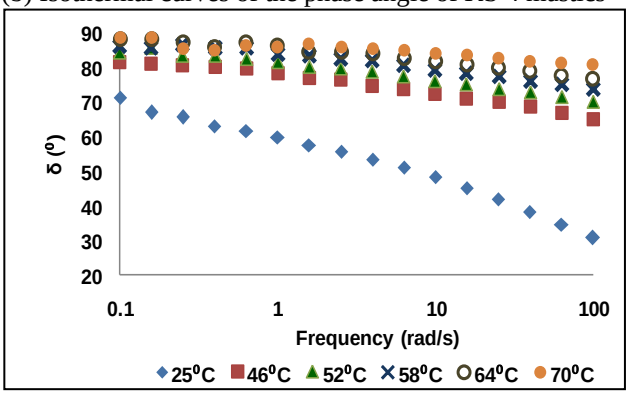

(d) Isothermal curves of the phase angle of GL 4 mastics

Figure 6.11 Isothermal curves of the phase angle of mastics corresponding to 4% filler

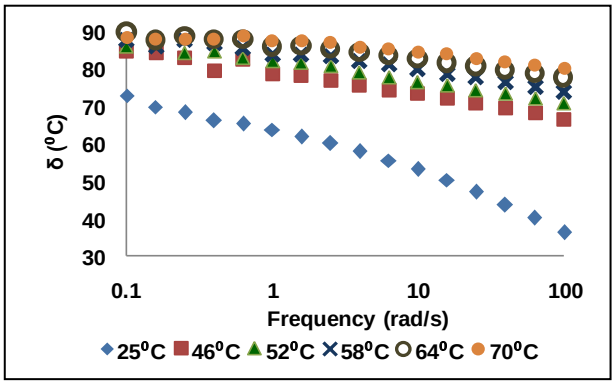

(a) Isothermal curves of phase angle of SD 5.5 mastics

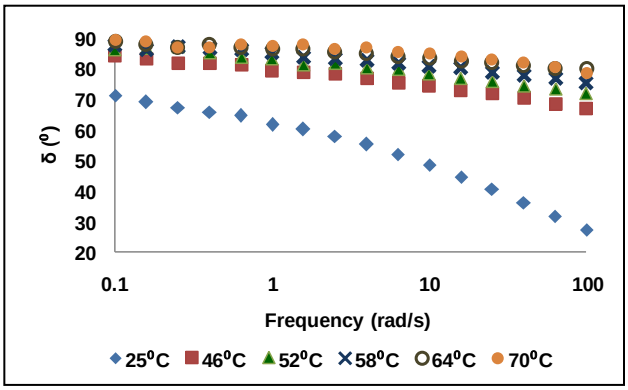

(b) Isothermal curves of phase angle of KS 5.5 mastics

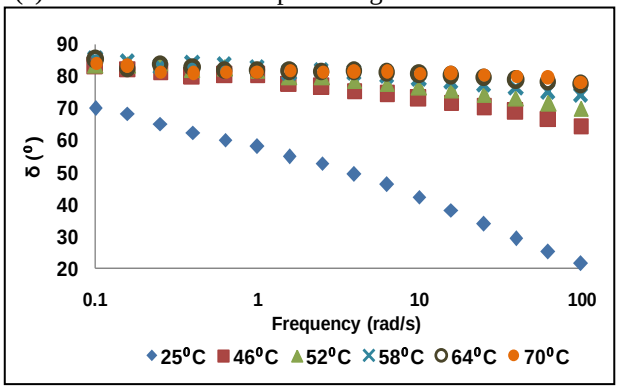

(c) Isothermal curves of phase angle of GP 5.5 mastics

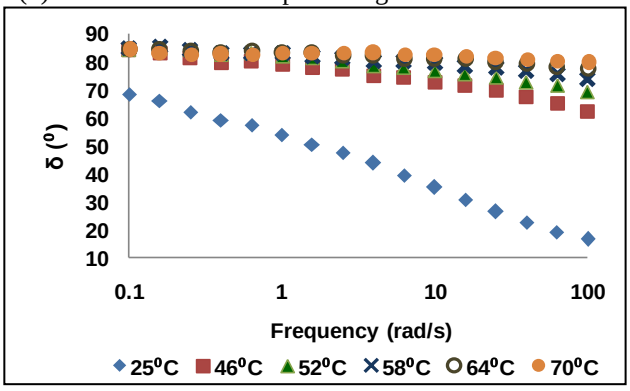

(d) Complex shear modulus of GL 5.5 mastics

Figure 6.12 Isothermal curves of the phase angle of mastics corresponding to 5.5% filler

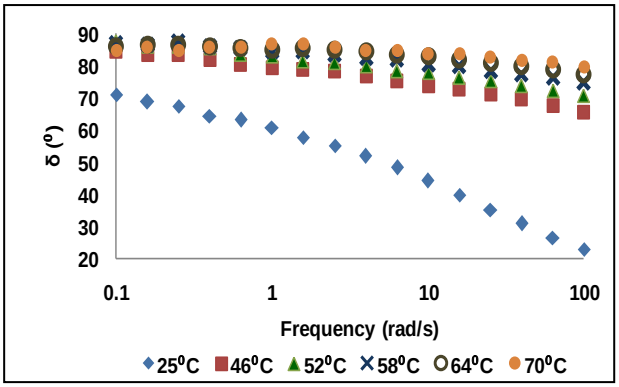

(a) Isothermal curves of the phase angle of SD 7 mastics

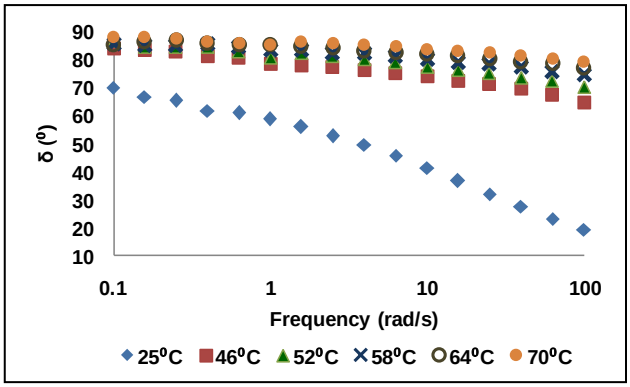

(b) Isothermal curves of the phase angle of KS 7 mastics

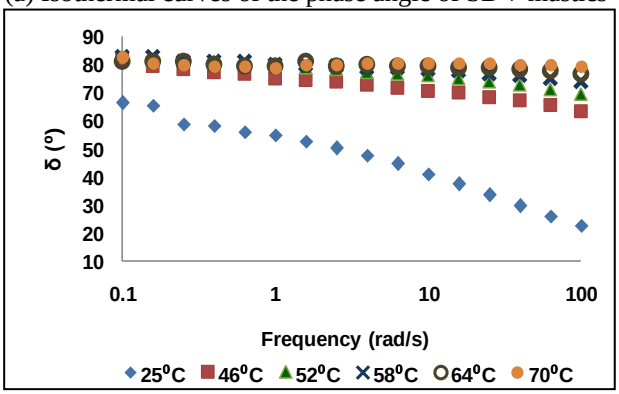

(c) Isothermal curves of the phase angle of GP 7 mastics

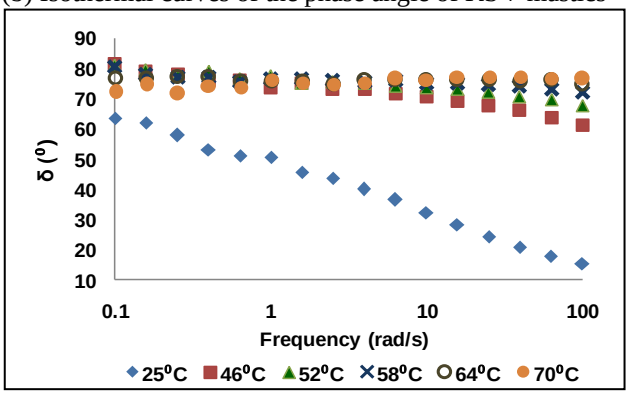

(d) Isothermal curves of the phase angle of GL 7 mastics

Figure 6.13 Isothermal curves of the phase angle of mastics corresponding to 7% filler

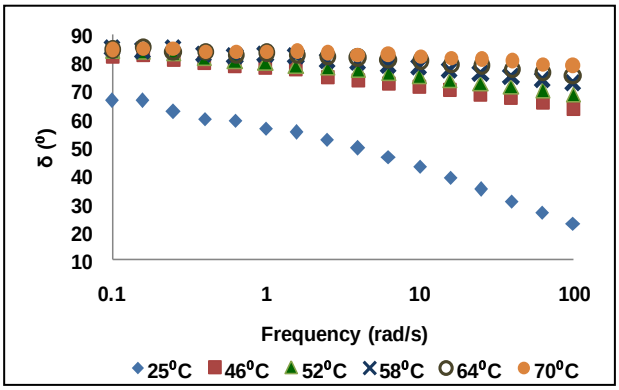

(a) Isothermal curves of phase angle of SD 8.5 mastics

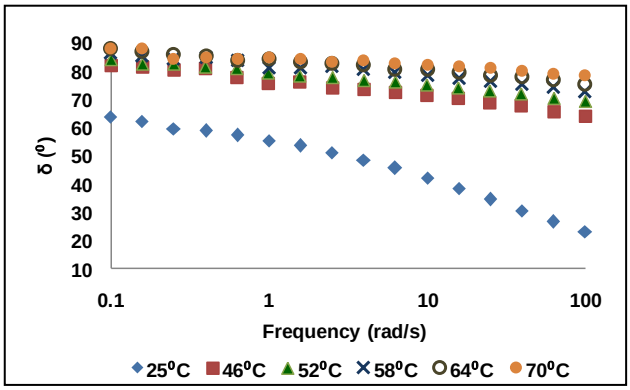

(b) Isothermal curves of phase angle of KS 8.5 mastics

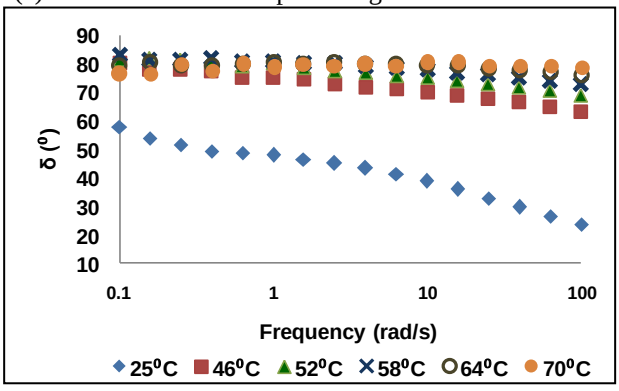

(c) Isothermal curves of phase angle of GP 8.5 mastics

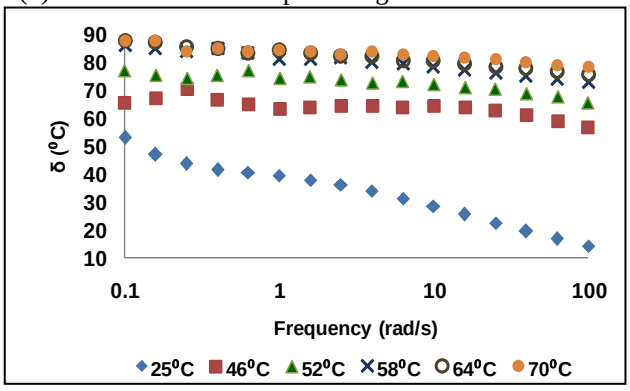

(d) Isothermal curves of phase angle of GL 8.5 mastics

Figure 6.14 Isothermal curves of the phase angle of mastics corresponding to 8.5% filler

Table 6.4 Rate of increase of complex shear modulus with the frequency (slope)

Type of Mastic	Rate of Increase in Complex Shear Modulus with Frequency (slope), at Different Temperatures					
	25°C	46°C	52°C	58°C	64°C	70°C
Bitumen	0.662	0.861	0.894	0.923	0.946	0.946
SD 4	0.657	0.852	0.886	0.917	0.942	0.951
SD 5.5	0.618	0.798	0.834	0.863	0.901	0.924
SD 7	0.577	0.849	0.888	0.904	0.927	0.936
SD 8.5	0.546	0.829	0.860	0.880	0.899	0.906
GP 4	0.614	0.834	0.869	0.911	0.920	0.945
GP 5.5	0.562	0.835	0.869	0.889	0.890	0.894
GP 7	0.521	0.777	0.847	0.863	0.852	0.838
GP 8.5	0.456	0.773	0.837	0.859	0.863	0.857
KS 4	0.623	0.841	0.876	0.913	0.937	0.950
KS 5.5	0.616	0.853	0.887	0.912	0.936	0.967
KS 7	0.550	0.848	0.885	0.909	0.920	0.939
KS 8.5	0.526	0.823	0.855	0.884	0.901	0.910
GL 4	0.594	0.833	0.875	0.902	0.929	0.934
GL 5.5	0.488	0.836	0.867	0.888	0.884	0.887
GL 7	0.436	0.800	0.821	0.820	0.811	0.791
GL 8.5	0.368	0.606	0.805	0.831	0.825	0.809

Table 6.5 Rate of decrease of phase angle with the frequency (slope)

Type of Mastic	Rate of Decrease in Phase Angle with Frequency (slope), at Different Temperatures					
	25°C	46°C	52°C	58°C	64°C	70°C
Bitumen	8.84	5.51	4.78	4.16	3.00	2.67
SD 4	11.14	6.11	5.09	4.59	4.01	2.52
SD 5.5	11.90	5.93	6.04	4.27	4.58	3.96
SD 7	15.36	6.41	5.48	4.16	2.92	2.09
SD 8.5	14.54	6.13	5.18	4.14	2.95	2.14
GP 4	14.10	6.42	5.73	4.69	2.92	2.21
GP 5.5	16.19	6.18	4.53	3.81	2.59	1.93
GP 7	14.53	6.22	4.49	2.96	1.43	0.10
GP 8.5	11.42	5.66	4.17	3.38	1.15	-
KS 4	14.10	6.33	5.27	4.46	3.54	2.47
KS 5.5	14.70	5.89	4.84	4.05	3.09	3.57
KS 7	16.84	6.43	5.35	3.67	2.70	3.05
KS 8.5	13.64	6.02	5.03	4.45	4.18	1.55
GL 4	13.53	5.45	5.19	4.09	3.87	2.59
GL 5.5	17.34	7.37	5.03	3.65	1.59	1.25
GL 7	15.99	6.73	4.42	2.82	0.66	-
GL 8.5	12.90	3.50	3.85	2.45	0.05	0.59

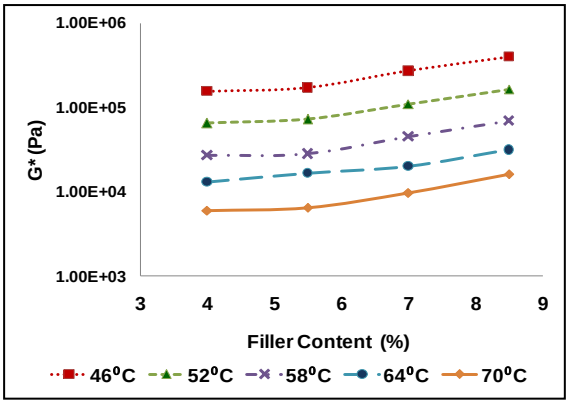

(a) Complex modulus of SD mastics at 10rad/s

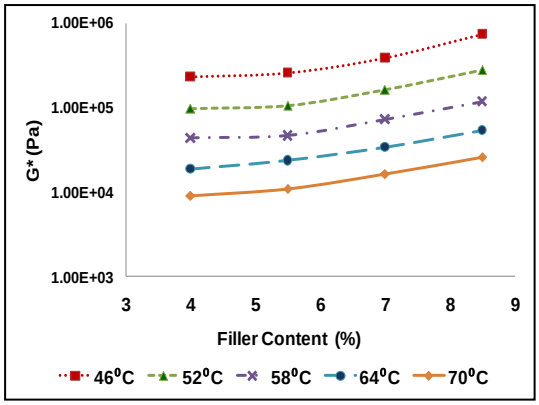

(b) Complex modulus of GP mastics at 10rad/s

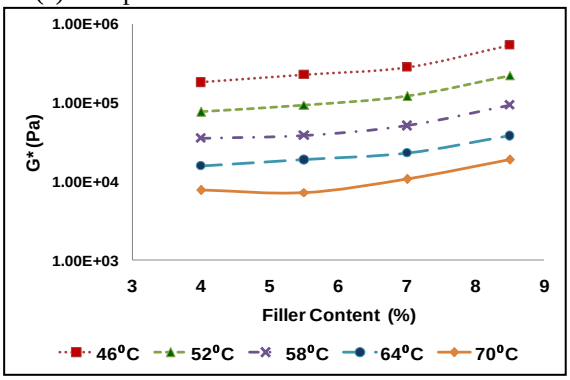

(c) Complex modulus of KS mastics at 10rad/s

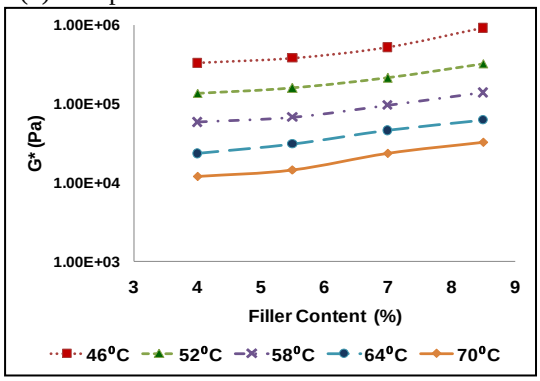

(d) Complex modulus of GL mastics at 10rad/s

Figure 6.15 Complex modulus of various mastics at 10rad/s

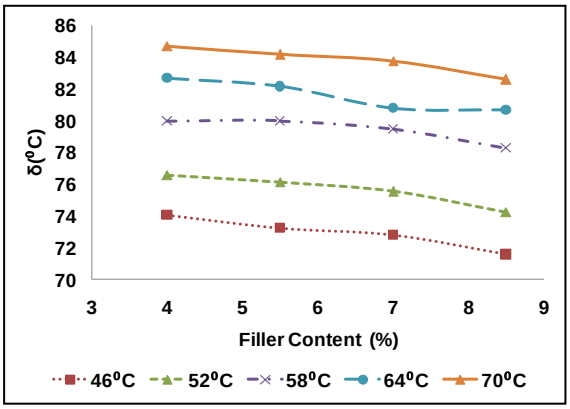

(a) Phase angle of SD mastics at 10rad/s

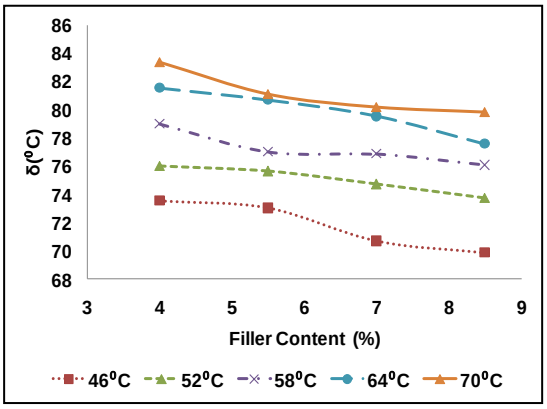

(b) Phase angle of GP mastics at 10rad/s

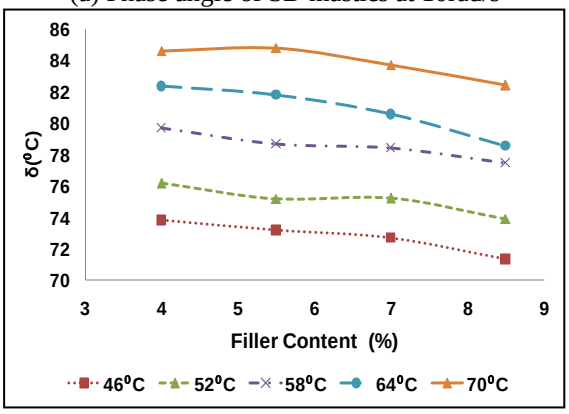

(c) Phase angle of KS mastics at 10rad/s

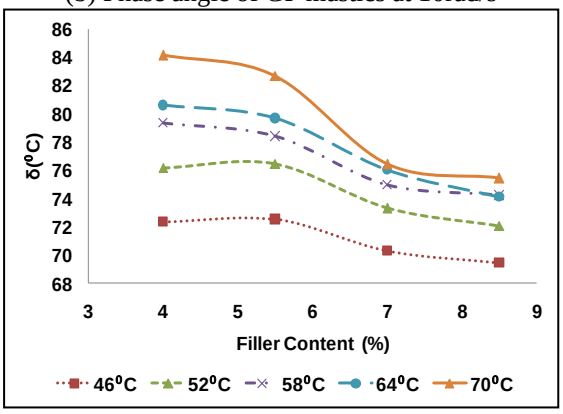

(d) Phase angle of GL mastics at 10rad/s

Figure 6.16 Phase angle of various mastics at 10 rad/s

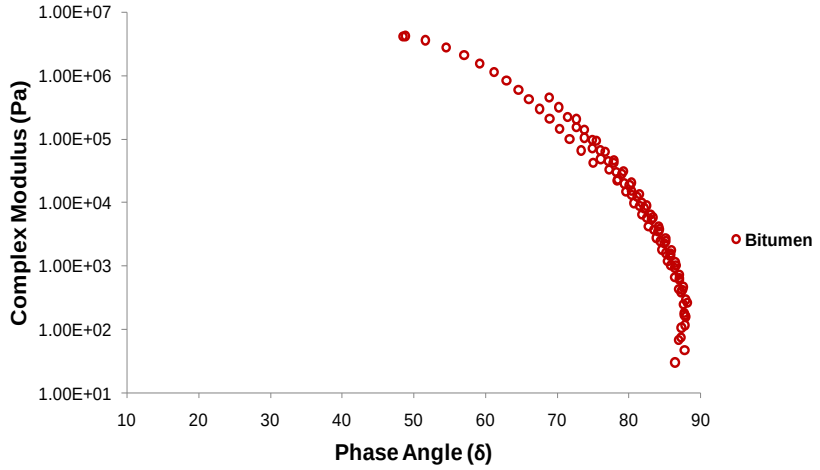

(a) Black diagram of pure bitumen

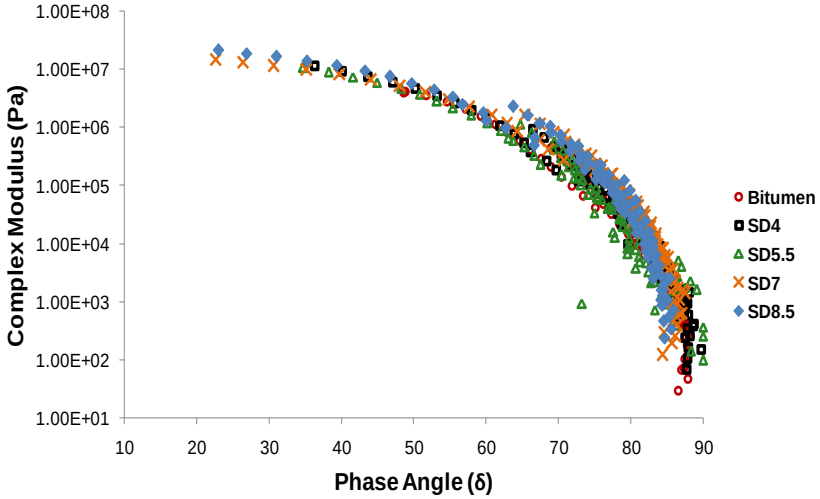

(b) Black diagram of SD mastics

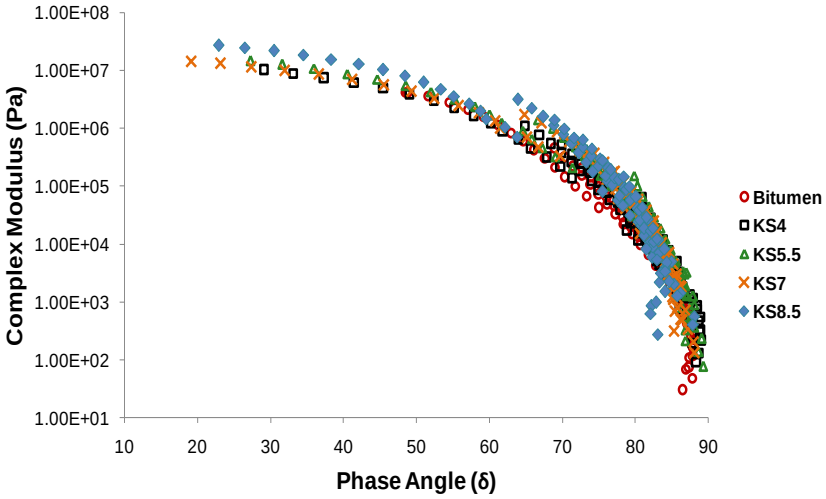

(c) Black diagram of KS mastics

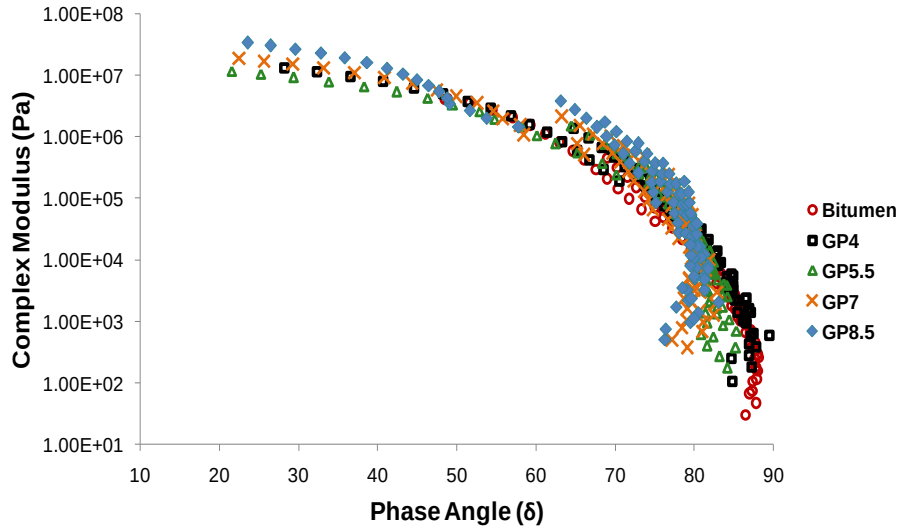

(d) Black diagram of GP mastics

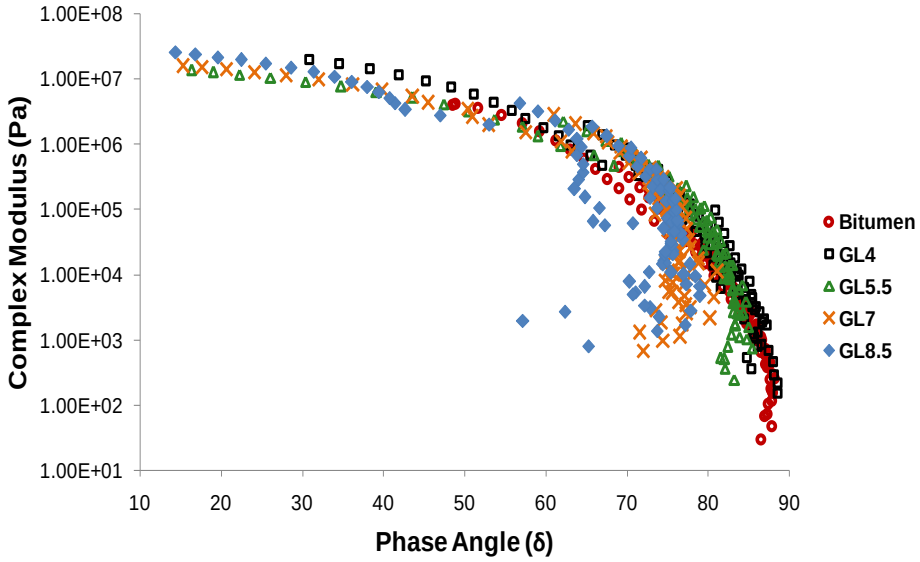

(e) Black diagram of GL mastics

Figure 6.17 Black diagrams of bitumen and mastics

6.5.6 Performance Evaluation of Bitumen and Mastics

6.5.6.1 *Rutting Resistance*

In case of bitumen and bituminous mastics, rutting can be defined as the accumulation of the non-recoverable (viscous) component of the responses to repeated load applications at high temperatures (Baustista, 2015). The analyses were performed on short-term aged mastic that corresponds to the early age of bitumen and mastics, i.e.,

immediately after its placement and before the start of oxidative ageing. This study characterized rutting resistance of bituminous mastics using Superpave protocol and MSCR tests. Although these tests were not developed to characterize the mastics, they were referred in this study for characterization and comparison of various mastics. Hence, Superpave rutting parameter ($G^*/\sin\delta$) was used for quantitative and qualitative analysis of various mastics but limits specified by Superpave protocol (SP-1, 2003) were not adhered (Bautista, 2015; Das and Singh, 2017; Kim et al., 2003).

Several studies have reported the inability of rutting parameter to characterize the permanent deformation characteristics of modified bitumen and mastics (Bahia et al., 2001; Bouldin et al., 2001; Carswell and Green, 2000; Dongre and D'Angelo, 2003). Superpave rutting parameter was devised to analyze the unmodified bitumen in linear viscoelastic domain. Hence it is not apposite to analyze mastics which are non homogenous in nature and has non linearity associated with it at higher temperatures and stress levels. Hence Multiple Stress Creep and Recovery (MSCR) test was also performed in addition to the analysis of Superpave rutting parameter for determination of rutting resistance in both linear and non-linear viscoelastic domain.

6.5.6.1.1 *Superpave Rutting Parameter*

For each cycle of sinusoidal traffic loading, some work is done to deform the bituminous pavement surface. A part of this work is recovered in the form of elastic rebound of the surface while other is dissipated in the form of permanent deformation (rutting) or heat. The work dissipated per loading cycle can be mathematically represented as Equation 6.4,

$$W_c = \pi \times \sigma^2 \times \left[\frac{1}{\frac{G*}{sin\delta}}\right] \quad [6.4]$$

Where: W_c = Work dissipated per load cycle

σ = Stress applied per load cycle

$G*$ = Complex shear modulus

δ = Phase shift angle

To ensure the minimum rutting resistance, the amount of dissipated work should also be minimized, which can be done by maximizing the value of G*/sinδ which is also known as rutting parameter. Hence higher value of G* and lower value of δ is preferred to design rut resistant mixes. The rutting parameter of various short-term aged mastics were determined at the temperature range of 46-70ºC and frequency range of 0.1-100 rad/s by performing frequency sweep test at linear viscoelastic region. The variation of rutting parameters with the loading frequency is stated in Figures 6.18-6.22. It can be seen that rutting parameter increased with the frequency and decrease with the temperature. Results clearly indicated that the inclusion of filler in the mastic tends to increase its rutting resistance. The rutting resistance of GL mastics was found to be highest followed by GP, KS, and SD mastics.

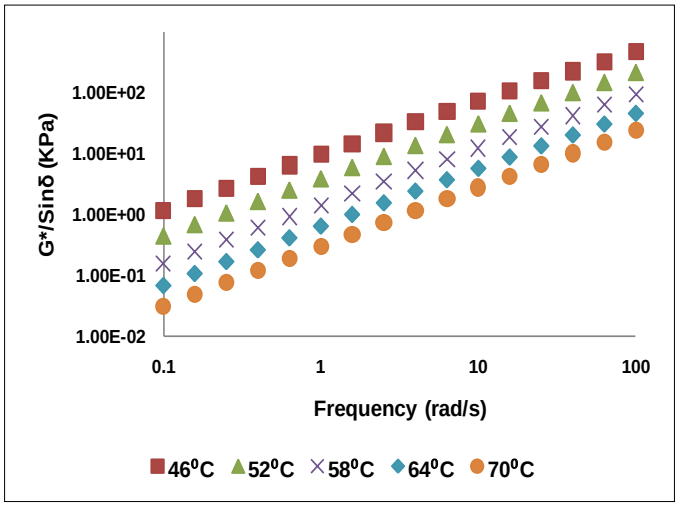

Figure 6.18 Variation of rutting parameters with frequency for bitumen

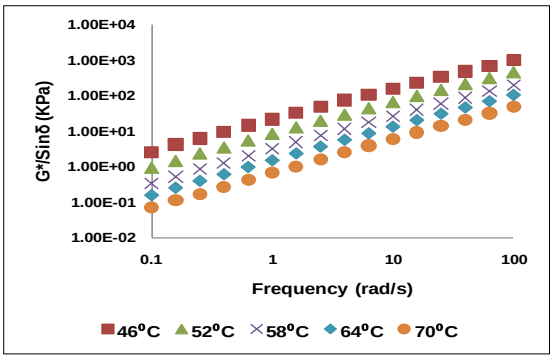

(a) Variation of rutting parameter with frequency for SD4 mastics

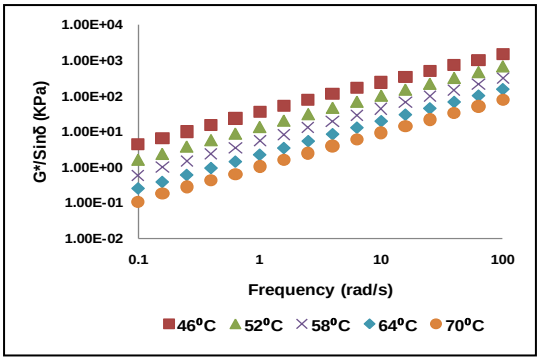

(b) Variation of rutting parameter with frequency for GP4 mastics

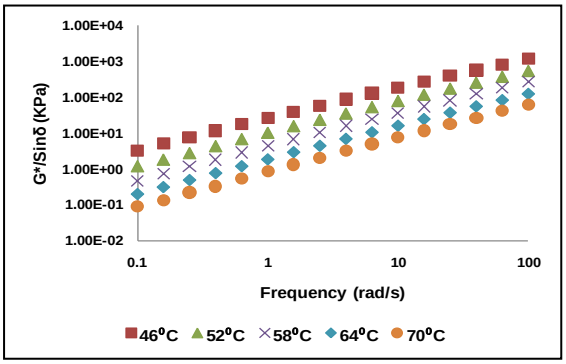

(c) Variation of rutting parameter with frequency for KS4 mastics

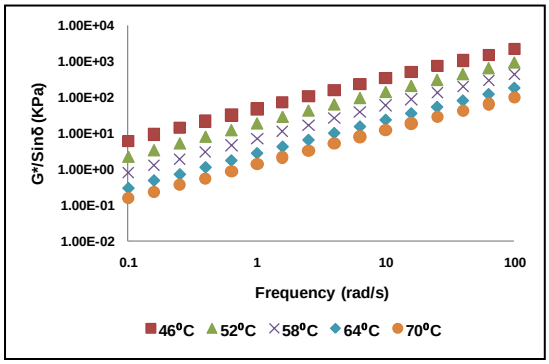

(d) Variation of rutting parameter with frequency for GL4 mastics

Figure 6.19 Variation of rutting parameters with frequency for mastics at 4% filler

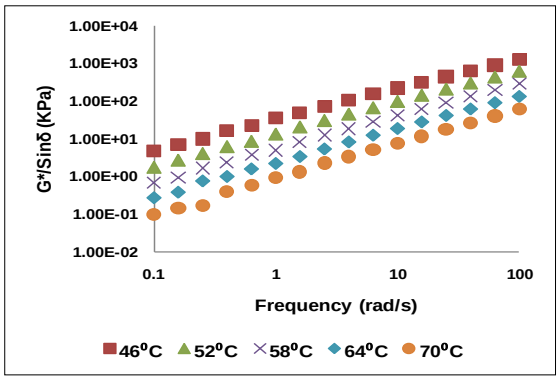

(a) Variation of rutting parameter with frequency for SD 5.5 mastics

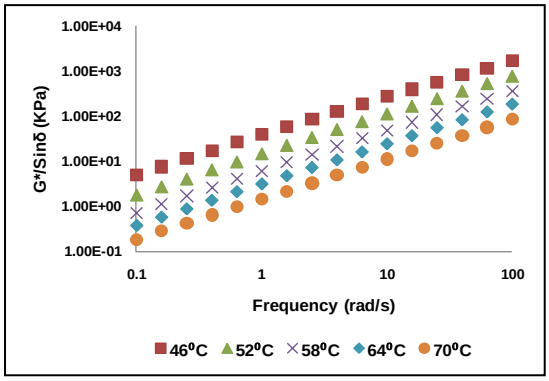

(b) Variation of rutting parameter with frequency for GP 5.5 mastics

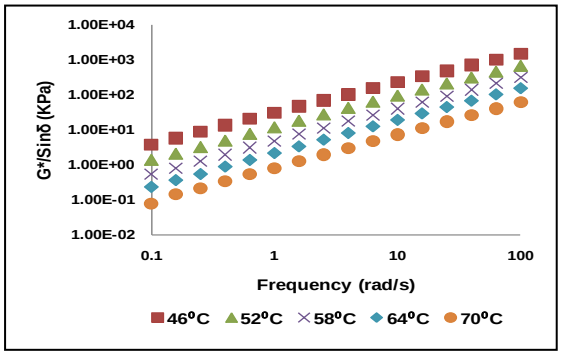

(c) Variation of rutting parameter with frequency for KS 5.5 mastics

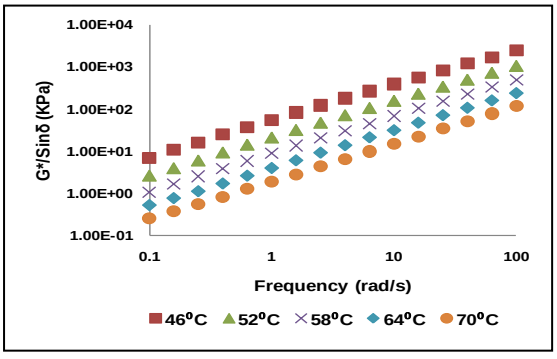

(d) Variation of rutting parameter with frequency for GL5.5 mastics

Figure 6.20 Variation of rutting parameters with frequency for mastics at 5.5% filler

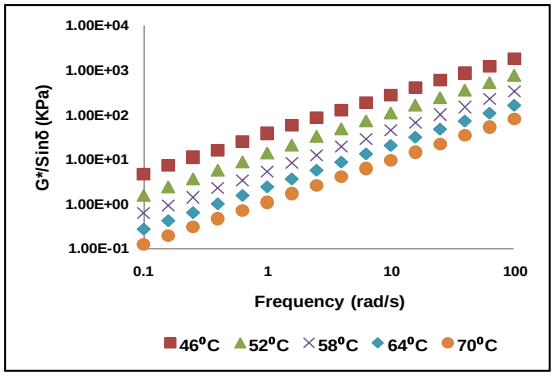

(a) Variation of rutting parameter with frequency for SD 7 mastics

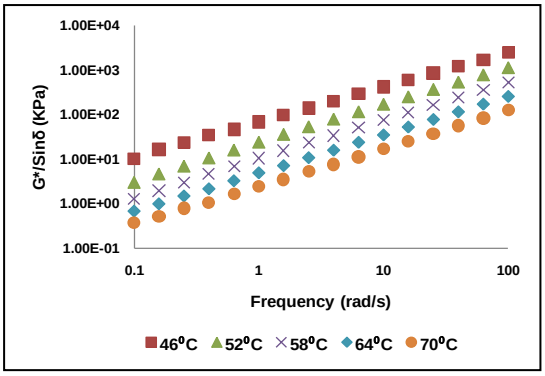

(b) Variation of rutting parameter with frequency for GP 7 mastics

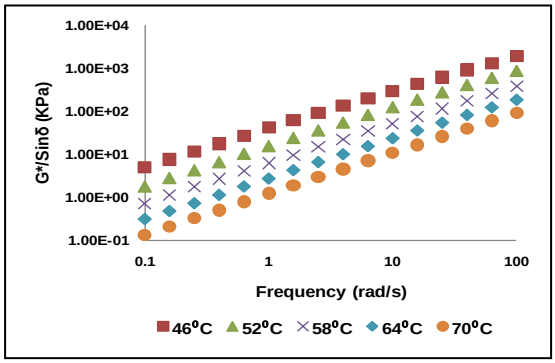

(c) Variation of rutting parameter with frequency for KS 7 mastics

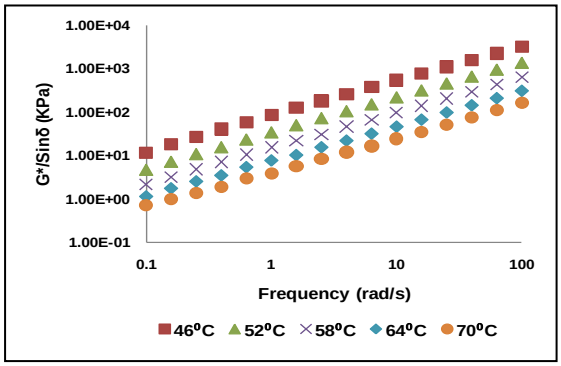

(d) Variation of rutting parameter with frequency for GL 7 mastics

Figure 6.21 Variation of rutting parameters with frequency for mastics at 7% filler

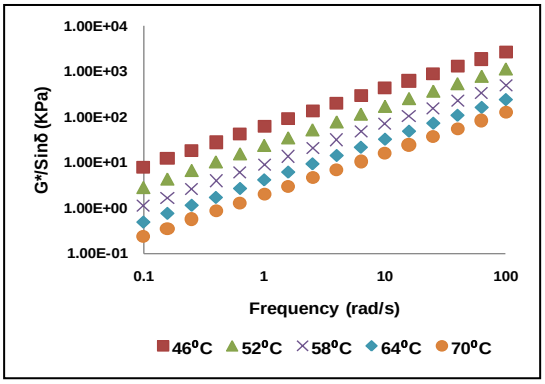

(a) Variation of rutting parameter with frequency for SD 8.5 mastics

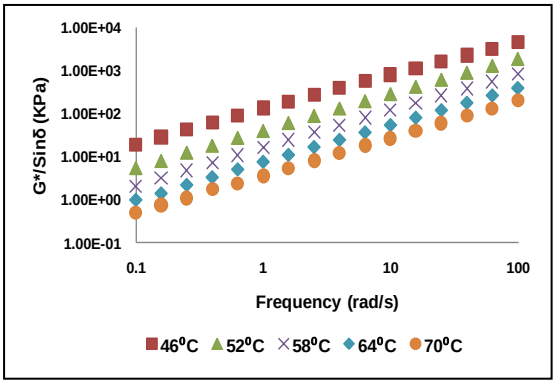

(b) Variation of rutting parameter with frequency for GP 8.5 mastics

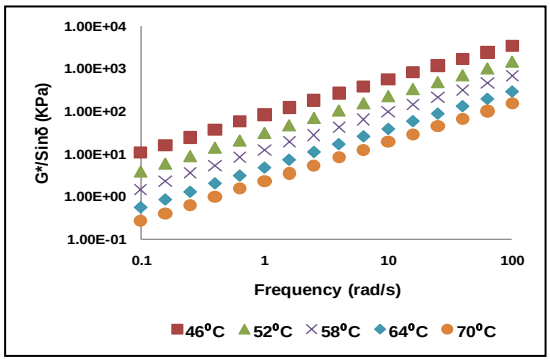

(c) Variation of rutting parameter with frequency for KS 8.5 mastics

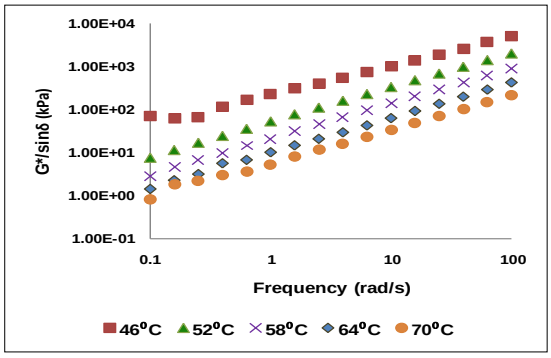

(d) Variation of rutting parameter with frequency for GL 8.5 mastics

Figure 6.22 Variation of rutting parameters with frequency for mastics at 8.5% filler

The comparison of rutting parameters is also done at the temperature of 64°C and at three different frequencies (0.1, 1, and 10 rad/s) (Table 6.6). At the test temperature of 64°C, the effect of frequency on G* is significant, whereas the phase angle is only affected marginally. Overall the rutting parameter was significantly increased with the frequency. However, in general, it is interesting to observe that the ratio of rutting parameter at higher frequencies (1 and 10 rad/s) to that at lower frequency (0.1 rad/s) reduces with the increase in stiffness of mastic. Hence rutting resistance of mastics prepared with higher filler content is less susceptible to the frequency change. Overall GL mastics were found to be less susceptible to the frequency followed by GP, GL, and SD. All mastics along with the bitumen were ranked in terms of their rutting resistance at 64°C and 10 rad/s and are stated in Table 6.6.

Table 6.6 Rutting parameters at 64°C and at three different frequencies

Frequency	0.1 rad/s			1 rad/s			10 rad/s		
Type of mastic	G* (kPa)	δ	G*/sinδ (kPa)	G* (kPa)	δ	G*/sinδ (kPa)	G* (kPa)	δ	G*/sinδ (kPa)
Bitumen	0.06	87.99	0.06	0.64	87.19	0.64	5.76	83.47	5.79
SD 4	0.15	87.69	0.15	1.46	83.82	1.47	12.98	82.67	13.09
SD 5.5	0.20	85.64	0.20	1.95	83.54	1.96	16.41	82.14	16.57
SD 7	0.26	84.68	0.26	2.32	82.74	2.34	19.81	80.77	20.07
SD 8.5	0.46	84.55	0.47	3.98	83.49	4.00	31.23	80.67	31.65
GP 4	0.25	86.5	0.25	2.21	82.62	2.23	18.93	81.55	19.13
GP 5.5	0.37	85.21	0.38	3.07	81.77	3.10	23.52	80.70	23.83
GP 7	0.67	81.08	0.68	4.81	79.39	4.89	33.76	79.54	34.33
GP 8.5	0.98	79.47	1.00	7.52	78.54	7.67	53.32	77.57	54.60
KS 4	0.19	87.10	0.19	1.79	83.02	1.80	15.75	82.34	15.89
KS 5.5	0.23	84.91	0.23	2.15	82.84	2.16	18.87	81.81	19.06
KS 7	0.31	83.10	0.31	2.68	82.17	2.71	23.00	80.56	23.31
KS 8.5	0.56	80.05	0.56	4.73	80.29	4.80	37.98	78.54	38.76
GL 4	0.29	84.10	0.29	2.72	81.7	2.75	23.10	80.60	23.41
GL 5.5	0.51	82.06	0.52	3.89	80.45	3.95	30.55	79.67	31.05
GL 7	1.12	76.58	1.15	7.56	75.71	7.80	45.45	76.02	46.84
GL 8.5	1.39	75.75	1.43	10.04	74.45	10.42	62.20	74.12	64.62

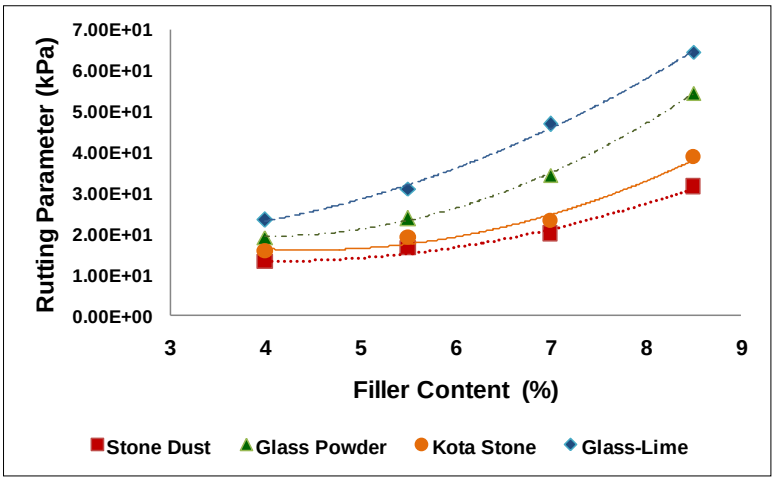

Figure 6.23 Rutting parameters of various mastics at 64°C and 10 rad/s

Figure 6.23 displayed the behaviour of mastics at the same temperature (64°C) and frequency (10 rad/s). It can be inferred that the rate of increase of rutting parameter increases with the filler content. The significant increase in the rate is observed in mastics corresponding to 7 and 8.5% filler content. This might be due to the higher interaction due to higher filler volume fraction in these mastics. This could also be noticed that GL mastics displayed higher variation in rutting parameter followed by GP, KS, and SD mastics. GL and SD mastics also had highest and lowest filler volume fraction respectively which validates the above specified hypothesis.

6.5.6.1.2 *Multiple Stress Creep and Recovery (MSCR) test*

The MSCR test calculates the rutting resistance of bituminous binders and mastics based on their delayed elasticity and accumulated strain. In this analysis, the specimen is subjected to specific magnitude of creep stress over a specified period of time followed by a recovery period. The specimen recovers a portion of strain during the recovery period. It subsequently used to calculate two important parameters known as non-recoverable creep compliance (J_{nr}) and percentage recovery (%R). J_{nr} refers to the ratio of the accumulated strain to the applied stress of the specimen and act an indicator of rutting resistance. Percentage recovery is the percentage of the total strain

recovered during the recovery period of the specimen. The response of the typical bitumen during the MSCR test is shown in Figure 6.24.

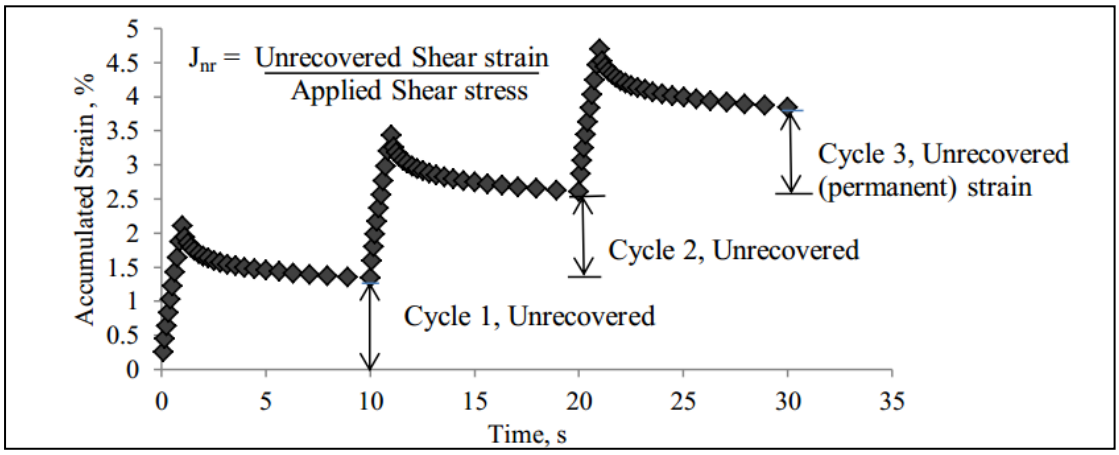

Figure 6.24 Variation of strain of bitumen during MSCR test

In this study, the MSCR test was conducted on short-term aged specimens according to AASHTO T350 specification using 25 mm diameter spindle and 1 mm gap between the parallel plates. It was done by repeated loading of bitumen and mastic specimens at the temperatures ranging from 46-70°C. The specimens were being subjected to 1s of creep loading and a 9s of recovery period at the stress levels of 0.1 and 3.2 kPa. The samples were subjected to 10 cycles for each stress level (Li et al., 2019; Rieksts et al., 2019). For each stress level, the average values for all 10 cycles were calculated and reported as J_{nr} and %R values. The specimen having lower J_{nr} at 3.2 kPa stress exhibited superior resistance against rutting, while %R value indicated the added elasticity in the modified bitumen and mastics. The stress sensitivity of the bitumen and mastics was determined using the parameter J_{nr}, diff. It was calculated by taking the ratio of the difference in J_{nr} determined at 0.1 and 3.2 kPa stress levels with the J_{nr} at 0.1 kPa stress. It is represented in form of percentage and specimen having higher J_{nr}, diff value signifies its higher stress sensitivity and vice versa.

Table 6.7 Average J_{nr} diff values (%) of different mastics

Type of mastic	Average J_{nr}, diff values (%) of mastics				
	46°C	52°C	58°C	64°C	70°C
Bitumen	13.76	16.00	20.43	26.18	33.36
SD 4	10.51	8.96	16.35	13.88	24.28
KS 4	7.43	13.53	12.16	17.49	18.89
GP 4	3.76	5.47	6.68	13.94	15.75
GL 4	6.67	8.90	1.74	20.23	8.80
SD 5.5	5.86	12.01	8.54	12.76	15.31
KS 5.5	6.52	1.76	7.00	15.42	20.58
GP 5.5	12.89	14.50	14.73	18.77	16.33
GL 5.5	4.61	17.21	24.04	21.14	24.99
SD 7	3.57	5.53	8.44	14.36	21.85
KS 7	4.25	7.20	4.52	10.28	21.98
GP 7	9.43	12.66	14.29	8.10	8.49
GL 7	1.54	1.78	9.52	8.99	2.45
SD 8.5	1.71	4.26	8.14	14.68	27.96
KS 8.5	1.57	5.65	7.37	9.78	16.56
GP 8.5	4.65	5.49	15.79	1.22	0.77

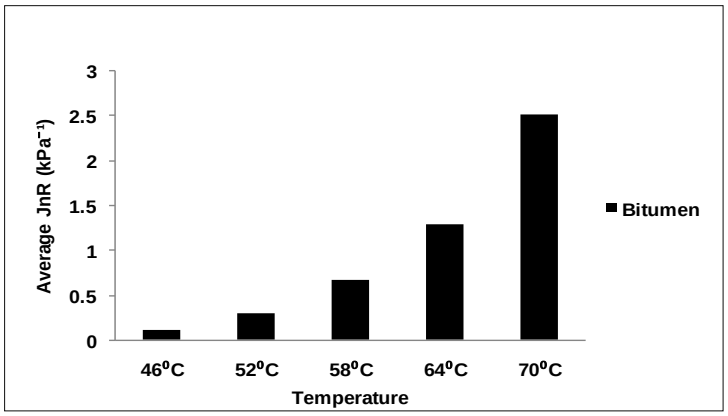

(a) J_{nr} values of bitumen at different temperatures at 0.1 kPa stress

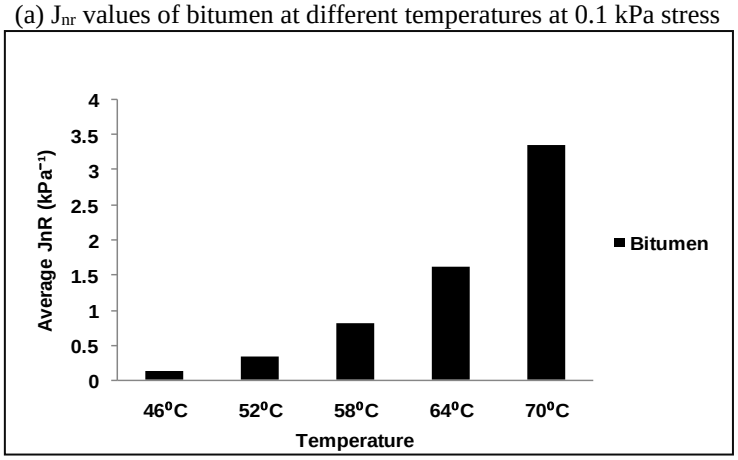

(b) J_{nr} values of bitumen at different temperatures at 3.2 kPa stress

Figure 6.25 J_{nr} values of bitumen at different temperatures at 0.1 and 3.2 kPa stresses

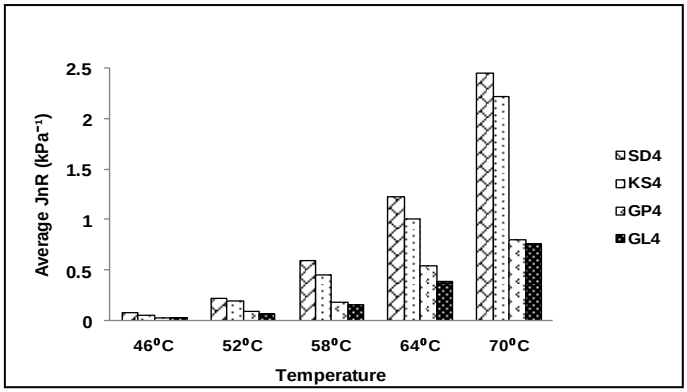

(a) J_{nr} values of mastics corresponding to 4% filler at different temperatures at 0.1 kPa stress

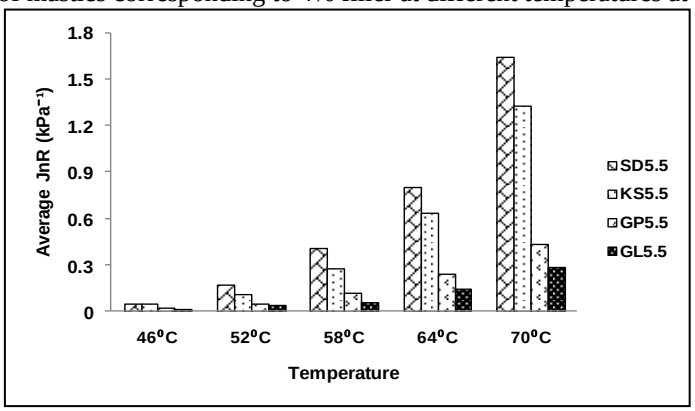

(b) J_{nr} values of mastics corresponding to 5.5% filler at different temperatures at 0.1 kPa stress

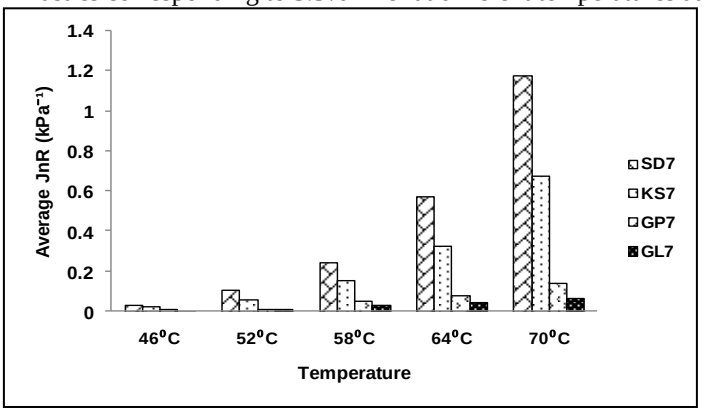

(c) J_{nr} values of mastics corresponding to 7% filler at different temperatures at 0.1 kPa stress

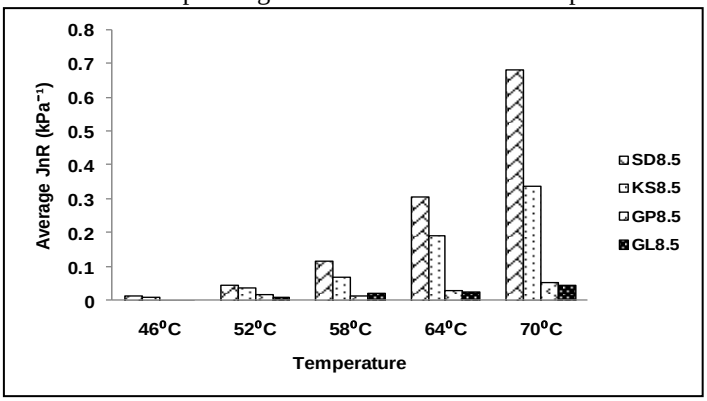

(d) J_{nr} values of mastics corresponding to 8.5% filler at different temperatures at 0.1 kPa stress

Figure 6.26 J_{nr} values of mastics at different temperatures at 0.1 kPa stress

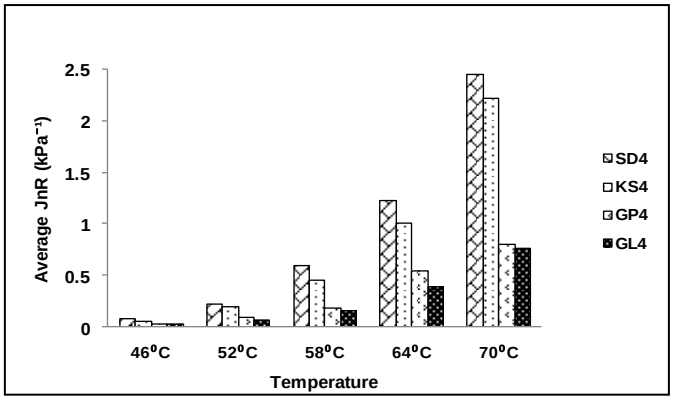

(a) J_{nr} values of mastics corresponding to 4% filler at different temperatures at 3.2 kPa stress

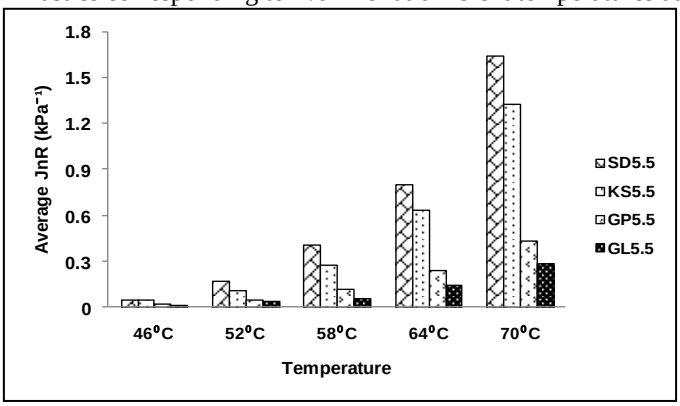

(b) J_{nr} values of mastics corresponding to 5.5% filler at different temperatures at 3.2 kPa stress

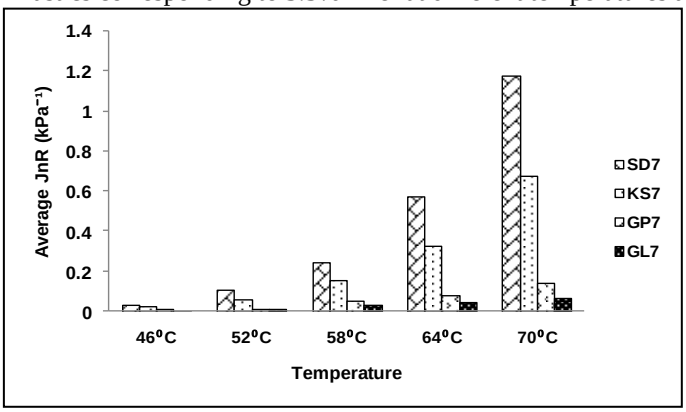

(c) J_{nr} values of mastics corresponding to 7% filler at different temperatures at 3.2 kPa stress

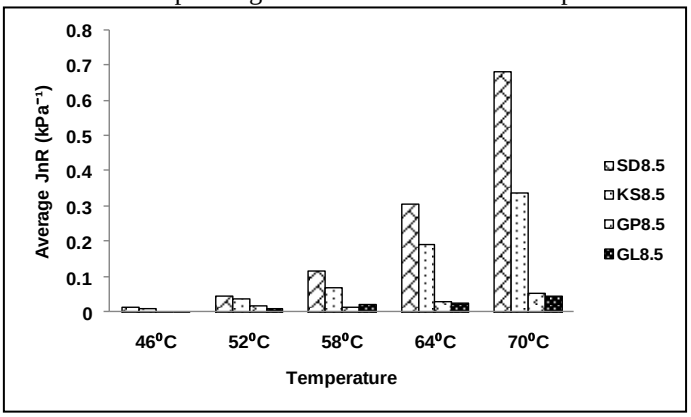

(d) J_{nr} values of mastics corresponding to 8.5% filler at different temperatures at 3.2 kPa stress

Figure 6.27 J_{nr} values of mastics at different temperatures at 3.2 kPa stress

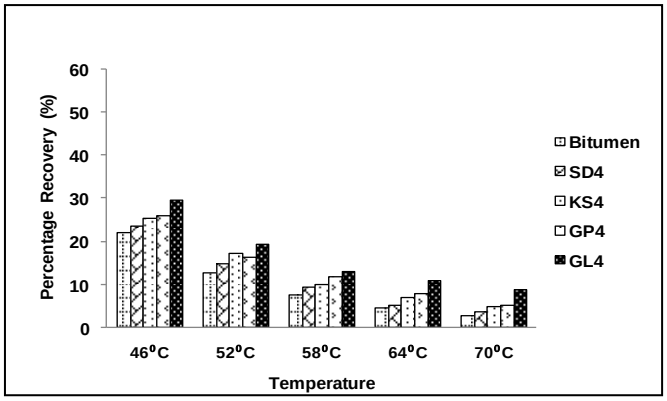

(a) Percentage Recovery (%) of bitumen and 4% filler mastic at different temperatures at 0.1 kPa stress

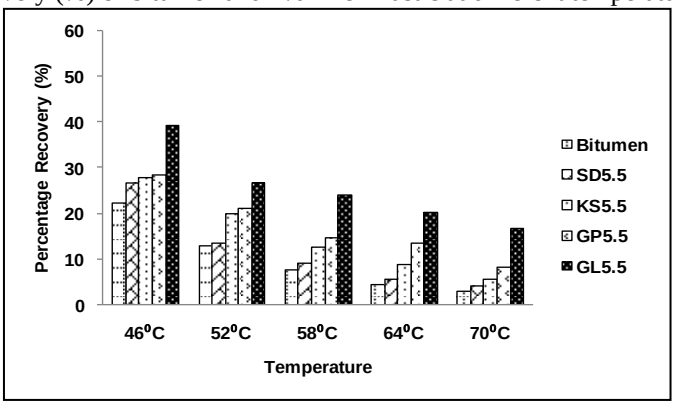

(b) Percentage Recovery (%) of bitumen and 5.5% filler mastic at different temperatures at 0.1 kPa stress

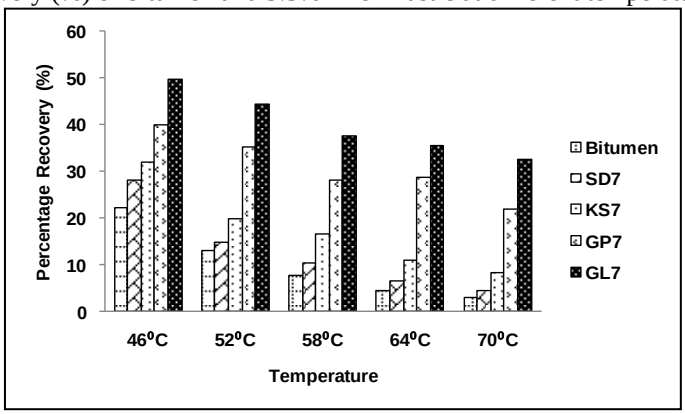

(c) Percentage Recovery (%) of bitumen and 7% filler mastic at different temperatures at 0.1 kPa stress

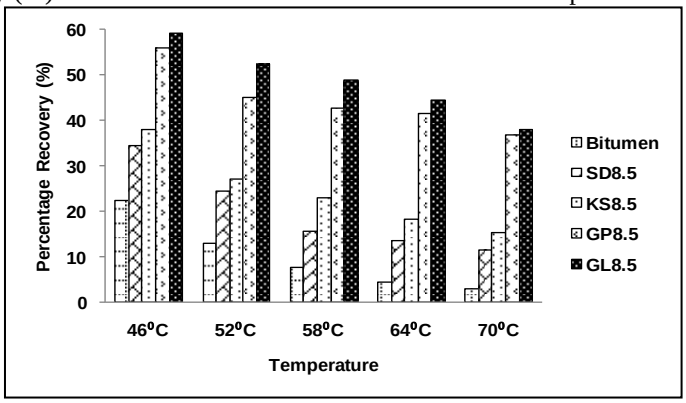

(d) Percentage Recovery (%) of bitumen and 8.5% filler mastic at different temperatures at 0.1 kPa stress

Figure 6.28 Percentage Recovery (%) of bitumen and mastics at different temperatures at 0.1 kPa stress

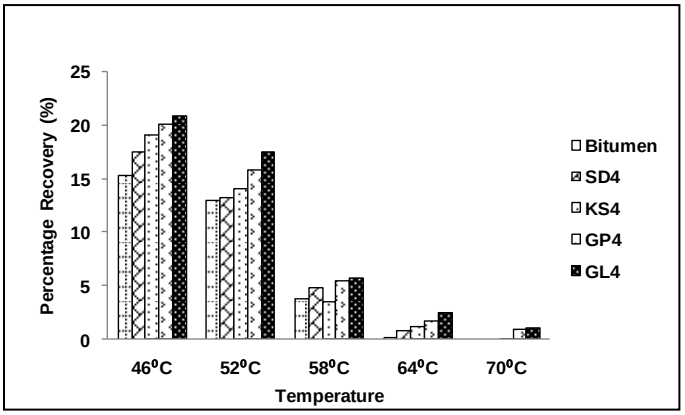

(a) Percentage Recovery (%) of bitumen and 4% filler mastic at different temperatures at 3.2 kPa stress

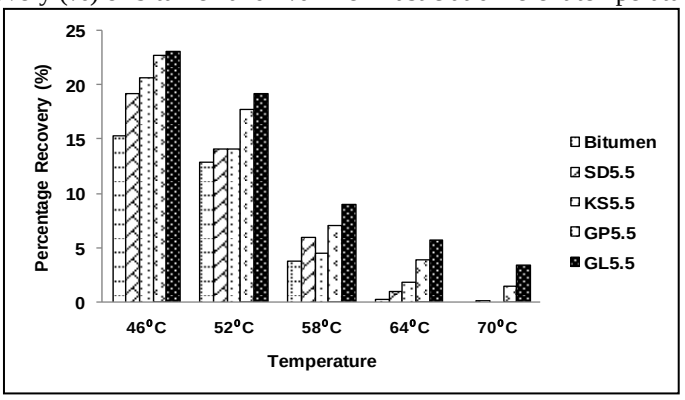

(b) Percentage Recovery (%) of bitumen and 5.5% filler mastic at different temperatures at 3.2 kPa stress

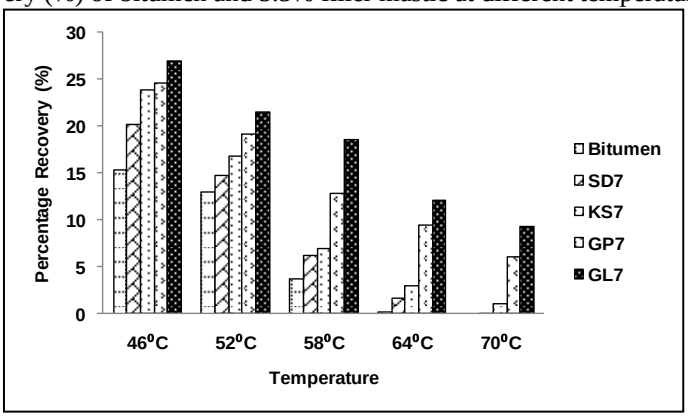

(c) Percentage Recovery (%) of bitumen and 7% filler mastic at different temperatures at 3.2 kPa stress

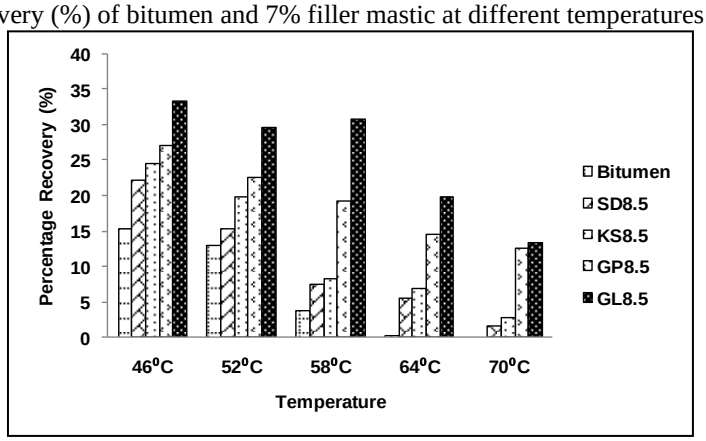

(d) Percentage Recovery (%) of bitumen and 8.5% filler mastic at different temperatures at 3.2 kPa stress

Figure 6.29 Percentage Recovery (%) of bitumen and mastics at different temperatures at 3.2 kPa stress

The J_{nr} values of bitumen and mastics at different temperatures and stress levels are shown in Figures 6.26-6.27, while the %R values are reported in Figures 6.28 and 6.29. The bitumen displayed highest J_{nr} values and lowest %R values, which indicated its relative inadequacy against rutting than mastics (Figure 6.24). In case of both bitumen and mastics, J_{nr} values increased with the increase in temperature, which is expected since bitumen behaves as viscous liquid at higher temperatures and exhibit higher rutting. J_{nr} values at both 0.1 and 3.2 kPa stress decreased with the increases in filler bitumen ratio (Figures 6.26-6.27). This indicated that the addition of filler volume leads to decrease in J_{nr} values and increased the rutting resistance of bituminous mastics. The magnitude of J_{nr} was also found to increase with increase in stress. It signified that the stress generated due to higher traffic loading lead to higher rutting in the bitumen and mastics. GL mastics displayed highest rutting resistance followed by GP, KS, and SD mastics. The ranking of bitumen and mastics was done in terms of their rutting resistance at 64°C using their J_{nr} values at 3.2 kPa stress levels. These ranking values are stated in Table 6.8 and were compared with the ranking values generated using rutting parameter at same temperature.

Percentage recovery (%R) is used to characterize the elasticity of the bitumen and mastics (Figures 6.28-6.29). The %R value of bitumen and mastics decreases with the increase in temperature. At higher stress level, the bitumen displayed negligible recovery at higher temperatures. The inclusion of filler volume imparted the elasticity in the mastics and hence %R was found to increase with filler bitumen ratio. The increase in filler volume in mastics absorbs the free bitumen and imparted the elastic nature to the mastic. The %R values at 3.2 kPa were found to be lower than 0.1 kPa. In general, the greater decrease in %R values with temperature was observed at higher

stress levels. Similar to the J_{nr} values, the %R values followed the similar trend with GL mastics displayed higher recovery followed by GP, KS, and SD mastics.

The J_{nr}, diff values of bitumen and various mastics are reported in Table 6.7, which is used to assess their sensitivity to stress. The continuous increase in J_{nr}, diff values of with the temperature reflected higher stress sensitivity of the bitumen and mastics with the increase in temperature. However, GP 8.5, GL 7, and GL 8.5 mastics deviated from this trend at higher temperatures. This might be due to the higher filler volume concentration in these mastics which inhibit the viscous behaviour of bitumen at higher temperature. This phenomenon needed further exploration and can be a part of a future study. The stress sensitivity of bitumen was found to be higher than the mastics. However, there is no well defined observable trend found between the filler content and the J_{nr}, diff values of the mastics.

Table 6.8 Ranking of mastics at 64°C with rutting parameter and MSCR

Type of mastic	Ranking of mastics at 64°C	
	Superpave rutting parameter	MSCR
Bitumen	17	17
SD 4	16	16
SD 5.5	14	14
SD 7	11	12
SD 8.5	6	8
GP 4	12	11
GP 5.5	8	7
GP 7	5	4
GP 8.5	2	2
KS4	15	15
KS 5.5	13	13
KS 7	10	9
KS 8.5	4	6
GL 4	9	10
GL 5.5	7	5
GL 7	3	3
GL 8.5	1	1

6.5.6.2 *Fatigue Resistance*

Fatigue cracking is one of the major distresses occurring on the pavement due to repeated load applications at intermediate service temperature. Fatigue cracking in pavements occurred during the later stage of its service life, hence, the analysis of fatigue in bitumen and mastic was done after subjecting them to short-term as well as long-term ageing. There is no well defined protocol for the determination of fatigue performance of mastics, hence protocols employed for bitumen are usually followed the relative assessment of mastics (Das and Singh, 2017; Das and Singh, 2018; Liao et al., 2012). In this section, the fatigue behavior of bitumen and mastics was analyzed at 25°C using Superpave fatigue parameter (G*sinδ), Linear Amplitude Sweep (LAS) test, and elastic recovery analysis using MSCR test.

6.5.6.2.1 *Superpave Fatigue Parameter*

The Superpave specification utilizes a stiffness based parameter known as fatigue parameter (G*sinδ) to analyze the fatigue damage of unmodified bitumen at low and intermediate temperatures. In DSR, the application of each cycle of oscillatory loading with "γ" magnitude strain, resulted in dissipation energy of magnitude $\pi\gamma^2$G*sinδ. Hence, damage accumulation can be minimized by lowering the dissipate energy per cycle which can be done by minimizing the parameter "G*sinδ". Hence low values of G* and δ are desirable from the standpoint of fatigue resistance. The fatigue parameter is measured at a fixed frequency (10 rad/s) with an applied strain well within the linear viscoelastic domain of bitumen and mastics. According to the Superpave guidelines (SP-1, 2003) the fatigue parameter of PAV aged bitumen should not exceed 5000 kPa. Since this limit of fatigue parameter is provided to characterize the unmodified bitumen and not mastics, the value of G*sinδ is used for the

comparison of mastics but the stated limit is not followed in the study. The bitumen and mastic were short-term aged initially, followed by the long-term ageing as per the protocols stated beforehand. The testing is conducted at 25°C and results are reported in Figure 6.30 and Table 6.9

Table 6.9 Complex modulus, phase angle and fatigue parameter of different mastics

Type of mastic	G* (kPa)	δ	G*sinδ (kPa)
Bitumen	1738	59.60	1499
SD 4	2334	54.37	1897
SD 5.5	3892	51.53	3047
SD 7	5300	48.67	3980
SD 8.5	8757	37.20	5294
GP 4	4399	48.71	3305
GP 5.5	6211	45.90	4460
GP 7	9442	38.50	5878
GP 8.5	12956	29.88	6454
KS 4	3582	51.74	2813
KS 5.5	4916	50.79	3809
KS 7	6746	41.22	4445
KS 8.5	10956	35.04	6290
GL 4	5576	45.11	3950
GL 5.5	10429	40.44	6765
GL 7	12602	32.96	6856
GL 8.5	14402	29.16	7017

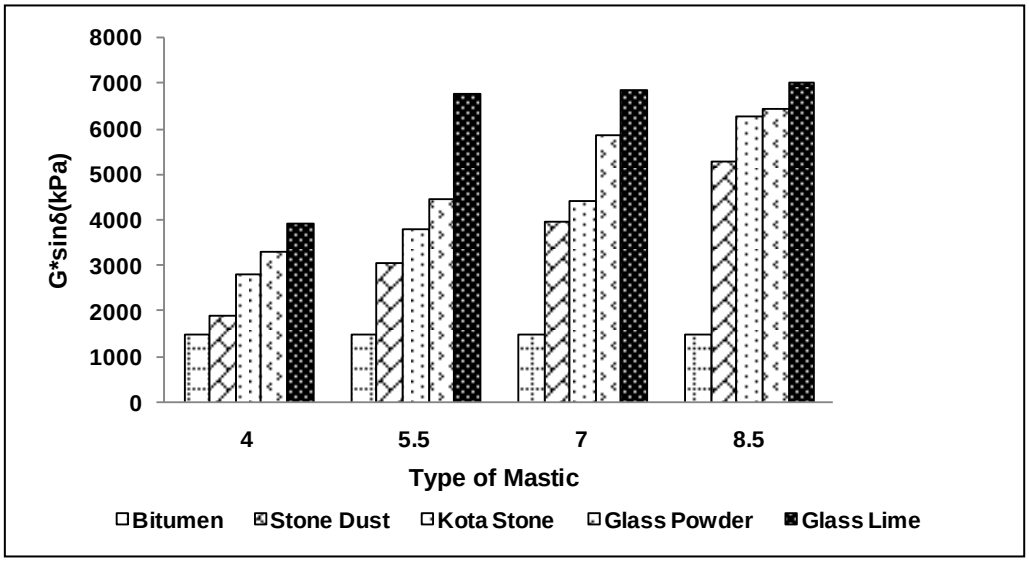

Figure 6.30 Fatigue parameter of bitumen and mastics at 25°C

It can be clearly seen that fatigue parameter increased with the increase in filler content in the mastics. It inferred that the fatigue resistance of the mastics decreased with the increase in filler content. This might be due to the increase in G* in the mastic due to the filler bitumen interaction caused by the higher filler volume concentration in the mastic. GL mastics were found to be more fatigue susceptible followed by GP, KS, and SD mastics. GL and GP mastics exceeded the bitumen specification ($G^*\sin\delta \leq 5000$ kPa) at the filler bitumen ratio corresponding to filler content of 5.5 and 7% respectively (GL 5.5 and GP 7 mastics). GL and GP also displayed higher rate of increase of fatigue parameter than SD and KS mastics. GL mastic observed a rapid increase in between GL 4 and GL 5.5, however the rate of increase dropped at the higher filler volume concentration. This increase might be due to the absorption of free bitumen within the mastic (due to higher porosity of GP and hydrated lime), which might have led to the increase in complex modulus in the mastic. GP also observed the higher rate of increase in between GP 5.5 and GP 7 mastics, while KS observed the similar increase in between KS 7 and KS 8.5 mastics. The conventional SD mastics displayed fairly similar rate of increase throughout the filler concentration. The ranking of various mastics against fatigue is shown in Table 6.12, however, it must be noted that this ranking is not conclusive since Superpave parameter analyzes the fatigue of the mastic only within the linear viscoelastic domain.

6.5.6.2.2 *Linear Amplitude Sweep*

The primary limitations of the analysis using fatigue parameter are that it analyzes the behavior of bitumen at single frequency and within linear viscoelastic domain. It doesn't explore the complicated fatigue behavior of bitumen and mastic occurred at

higher strain levels and at varied frequency. Hence to address the stated crucial issues, the fatigue behavior of mastics was also analyzed using Linear Amplitude Sweep test according to AASHTO TP 101-14 protocol. This test is based on Visco-Elastic Continuum Damage (VECD) principle and it evaluated the fatigue resistant ability of bitumen by providing cyclic loading at increasing amplitudes to accelerate damage. This analysis indicated the fatigue performance of bitumen for a given pavement structural condition and expected traffic loading using rate of damage accumulation and predictive modelling technique. This fatigue life of bitumen at different strain levels is dependent on two parameters A and B. These parameters were determined by conducting a frequency sweep test followed by a linear amplitude sweep. The frequency sweep test (0.2-30 Hz) is conducted at the strain level within linear viscoelastic domain (preferably 0.1%) to obtain undamaged material property (α) (Figure 6.31). The "α" is determined by taking the reciprocal of the straight line slope (m) of log G'(ω) versus log ω curve. Here, "G'(ω)" is the storage modulus of the specimen while, "ω" is the frequency of the testing. This "α" parameter is further utilized as an input parameter for the analysis in amplitude sweep test.

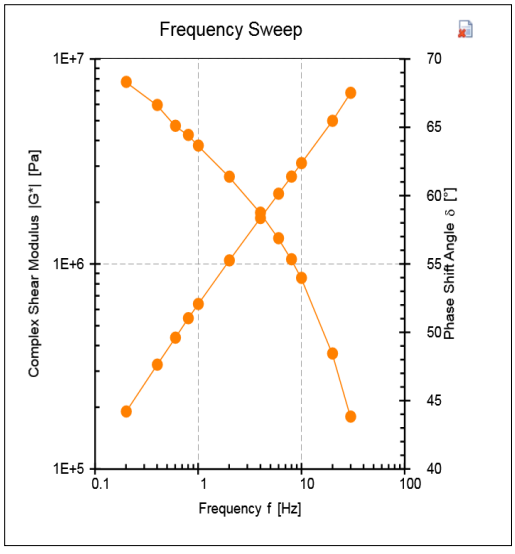

Figure 6.31 Variation of complex shear modulus and phase angle with frequency

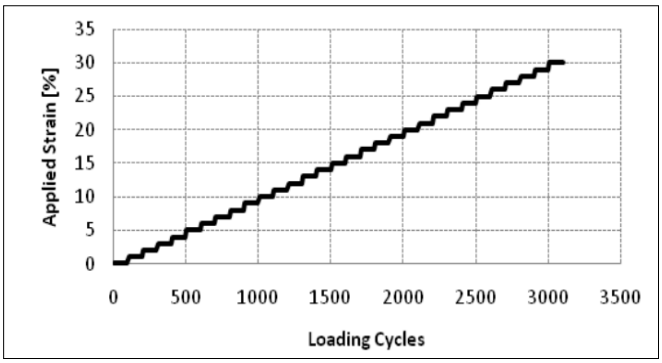

Figure 6.32 Loading scheme during amplitude sweep test (AASHTO TP 101-14)

The amplitude sweep test is conducted at 25°C in strain control mode at 10Hz frequency. The loading scheme comprised of constant strain amplitude applied at 10 second intervals, in which each interval is followed by another interval of increased strain amplitude. The loading scheme is shown in Figure 6.32 in which strain is varied from 0-30%, through 3100 loading cycles. The testing is done at sinusoidal loading with 100 cycles at each strain level; the rate of strain increment is taken as 1%.

The damage accumulation in the specimen is calculated using the formulae,

$$D(t) \cong \sum_{i=1}^{N} [\pi \gamma^2 (C_{i-1} - C_i)]^{\frac{\alpha}{1+\alpha}} (t_i - t_{i-1})^{\frac{1}{1+\alpha}} \quad [6.4]$$

Where, *C(t)* is also known as the integrity parameter and it is the ratio of $|G^*|(t)$ to $|G^*|_{initial}$, which are the values of complex shear modulus at any time "*t*" and the initial undamaged $|G^*|$

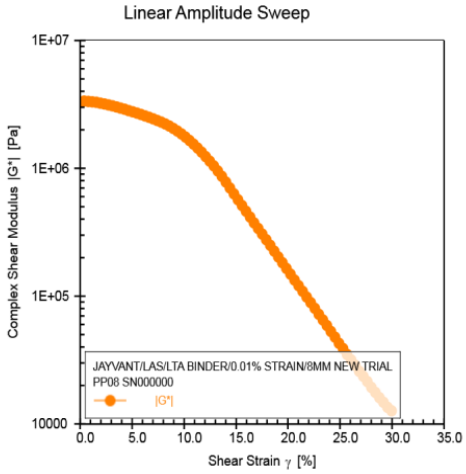

Figure 6.33 Variation of ($|G^*|(t)$) of bitumen with the strain

Further, the calculated *C(t)* and *D(t)* are used to fit a relationship in the form of

$$C_t = C_0 - C_1(D)^{C_2} \quad [6.5]$$

Where, C_0, C_1, and C_2 are evaluate using curve fitting, where C at peak stress is used to calculate the value of *D(t)* at failure (D_f) using the above equation. Figure 6.34 displayed the curve fitting between integrity parameter and damage accumulation of the bitumen.

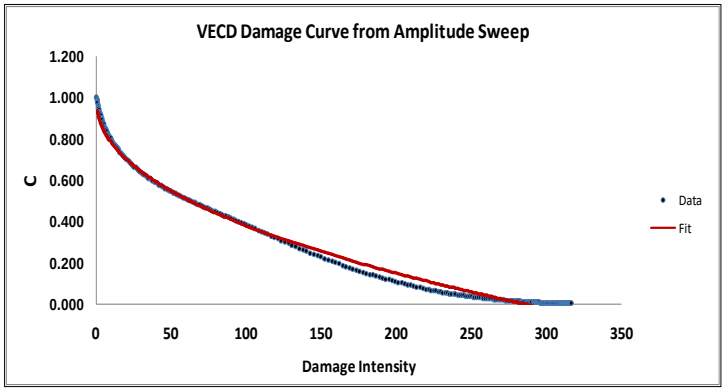

Figure 6.34 Curve fitting between integrity parameter and damage intensity of bitumen

The value of $D(t)$ at failure, D_f is stated as the $D(t)$ which corresponds to the reduction in initial |*G**| at peak shear stress, according to Equation 6.4.

$$D_f = \left(\frac{C_0 - C\ at\ peak\ stress}{C_1}\right)^{\frac{1}{C_2}} \quad [6.6]$$

The fatigue life (N_f) is calculated using the equation below

$$N_f = A(\gamma_{max})^B \quad [6.7]$$

Where, A and B are evaluated using the following equations

$$A = \frac{f(D_f)^k}{k(\pi C_1 C_2)^\alpha} \quad [6.8]$$

$$B = 2\alpha \quad [6.9]$$

In above Equations, *f* is the frequency (10 Hz) and *k* is calculated as follows

$$k = 1 + (1 - C_2)\alpha \quad [6.10]$$

Table 6.10 Fatigue damage parameters and fatigue life equations of bitumen and mastics

Type of mastic	α	C_1	C_2	A	B	$N_f = A(\gamma_{max})^B$
Bitumen	1.200	0.035	0.593	57830	-2.401	$N_f = 57830(\gamma_{max})^{-2.401}$
SD 4	1.257	0.062	0.519	23700	-2.514	$N_f = 23700(\gamma_{max})^{-2.514}$
GP 4	1.301	0.102	0.418	13900	-2.602	$N_f = 13900(\gamma_{max})^{-2.602}$
KS 4	1.263	0.076	0.457	27990	-2.526	$N_f = 27990(\gamma_{max})^{-2.526}$
GL 4	1.427	0.099	0.461	11690	-2.854	$N_f = 11690(\gamma_{max})^{-2.854}$
SD 5.5	1.231	0.088	0.426	20580	-2.462	$N_f = 20580(\gamma_{max})^{-2.462}$
GP 5.5	1.363	0.097	0.488	6754	-2.725	$N_f = 6754(\gamma_{max})^{-2.725}$
KS 5.5	1.256	0.082	0.463	16500	-2.513	$N_f = 16500(\gamma_{max})^{-2.513}$
GL 5.5	1.436	0.108	0.489	4958	-2.872	$N_f = 4958(\gamma_{max})^{-2.872}$
SD 7	1.383	0.085	0.532	7374	-2.766	$N_f = 7374(\gamma_{max})^{-2.766}$
GP 7	1.348	0.108	0.520	2560	-2.695	$N_f = 2560(\gamma_{max})^{-2.695}$
KS 7	1.336	0.139	0.375	5511	-2.671	$N_f = 5511(\gamma_{max})^{-2.671}$
GL 7	1.390	0.121	0.496	2289	-2.780	$N_f = 2289(\gamma_{max})^{-2.780}$
SD 8.5	1.448	0.119	0.484	3261	-2.896	$N_f = 3261(\gamma_{max})^{-2.896}$
GP 8.5	1.537	0.157	0.431	1852	-3.073	$N_f = 1852(\gamma_{max})^{-3.073}$
KS 8.5	1.418	0.151	0.428	1837	-2.836	$N_f = 1837(\gamma_{max})^{-2.836}$
GL 8.5	1.484	0.146	0.466	1606	-2.968	$N_f = 1606(\gamma_{max})^{-2.968}$

The fatigue damage parameters and fatigue life equation as obtained after the damage analysis of bitumen and mastics are shown in Table 6.10. The C_0 parameter was found to be 1 in all cases, which indicated the highest integrity with no damage. The fatigue life of bitumen and mastics are dependent on the parameters 'α' and 'A'. Parameter 'α' signifies the rate of reduction of fatigue with the increase in the amplitude of strain (Das and Singh, 2018; Saboo and Kumar, 2016). The parameter 'A' is directly proportional to the fatigue life as shown in Equation 6.7. Hence, higher value of 'A' and lower value of 'α' is necessary to ensure superior resistance of fatigue damage. The fatigue lives of bitumen and mastics are shown in Figure 6.35. The bitumen displayed the highest value of 'A' and lowest value of 'α' and hence exhibited highest fatigue life at all strain levels. In general, the decrease in 'α' with an increase in 'A' is displayed for all mastics with the increase in filler content. It can be implied that the increase in filler content tends to increase the fatigue susceptibility of the bituminous

mastics. This trend is more or less similar to that of Superpave fatigue parameter. The difference in fatigue lives of mastics is not predominant at lower strain levels, however, at higher strain levels, the difference in fatigue lives is noticeable especially in case of mastic corresponding lower filler concentration (4% and 5.5%).

The SD mastics displayed highest fatigue lives at all strain levels followed by KS, GP, and GL mastics. It seemed that the mastics due to higher filler volume content undergone brittle failure when higher amplitude of strain is applied. This can be also be observed by analyzing the slope between the fatigue life and strain amplitude (Figure 6.35). Fatigue life of GL and GP mastics decreased steeply at higher strain levels (typically after 2.5%), which suggested their higher strain susceptibility. However it can also be seen that mastics prepared at higher filler levels (7 and 8.5%) exhibited similar rate of decrease in fatigue life (similar slope throughout the strain levels) (Figure 6.35). It can be implied that the strain susceptibility of mastics decreased for the mastics having higher filler volume. Various studies have compared the fatigue life of the mastics at strain levels of 2.5 and 5% respectively (Das and Singh, 2017; Saboo and Kumar, 2016). The fatigue life of bitumen and all mastics was compared at 2.5% of strain level using the relationship given in Table 6.10 and presented in Figure 6.35. These fatigue lives were used to rank various mastics and determining their fatigue susceptibility. The ranking of various mastics is exhibited in Table 6.12.

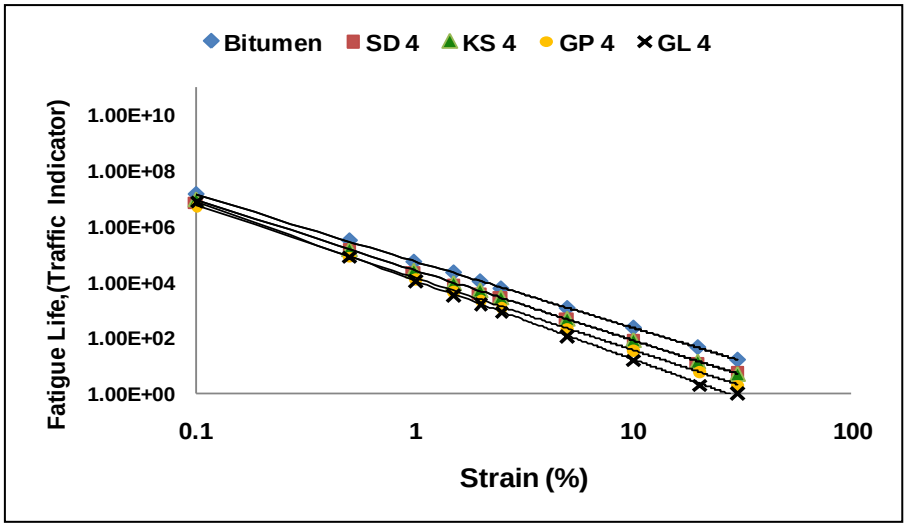

(a)Fatigue life of bitumen and 4% filler mastic at different strain levels

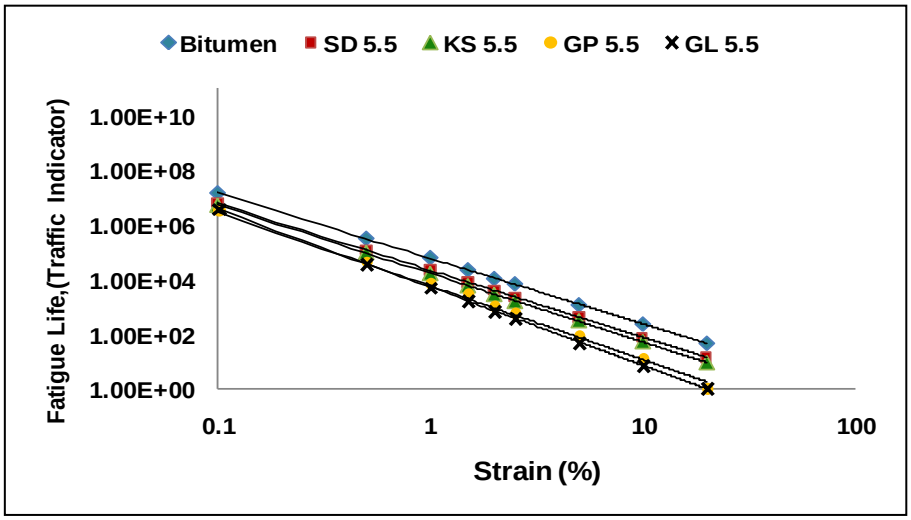

(b)Fatigue life of bitumen and 5.5% filler mastic at different strain levels

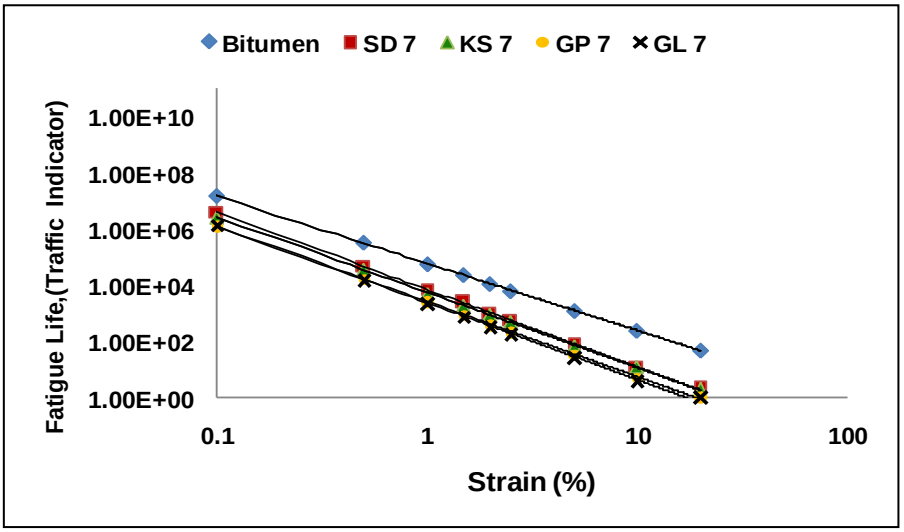

(c) Fatigue life of bitumen and 7% filler mastic

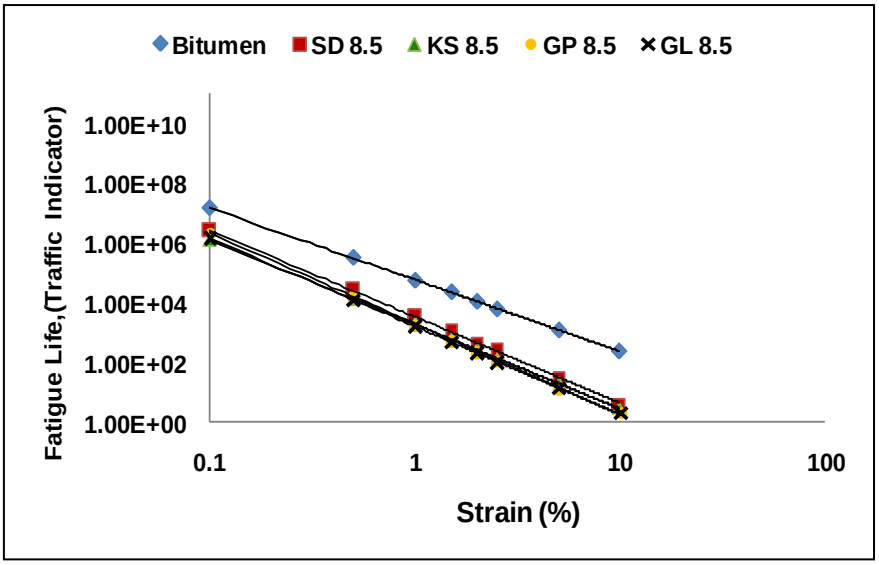

(d)Fatigue life of bitumen and 8.5% filler mastic

Figure 6.35 Fatigue life of bitumen and mastics at different strain levels

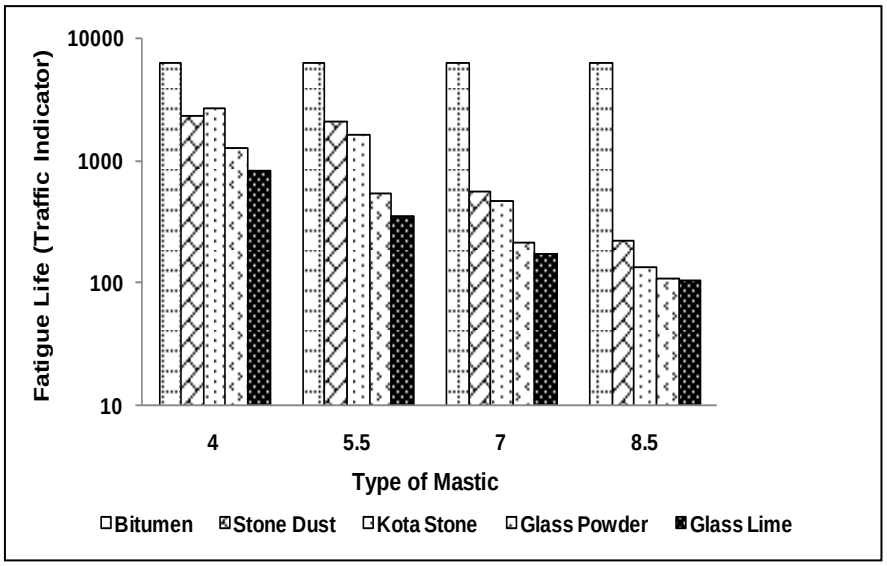

Figure 6.36 Fatigue life of various mastics at 2.5% strain

6.5.6.2.3 *Multiple Stress Creep and Recovery Test*

The MSCR test is primarily developed to characterize the rutting resistance of bitumen and it also has been used in this study to analyze the rutting resistance of mastics. However, recently MSCR has also been applied to quantify the fatigue resistance of bitumen (Zhang et al., 2018; Zhou et al., 2012). Percentage recovery (%R) determined from MSCR can potentially be used to evaluate the delayed elastic response of bitumen and mastics. It is hypothesized that the higher %R corresponds to

better fatigue resistance of bitumen and mastics. However it is a relatively new approach and no one has attempted to correlate the %R of long-term aged bituminous mastic at intermediate temperature (25°C) with the fatigue resistance of mastic.

In this analysis, the bitumen and mastic were short-term aged initially, followed by the long-term ageing as per the protocols stated before. The MSCR test was performed according to AASHTO T 350 protocol as suggested in the section 6.5.6.1.2. The testing was conducted at 25°C with 8 mm parallel plate geometry with 2 mm gap. Since J_{nr} and %R are well correlated, only the %R values of mastics were taken in the analysis. Furthermore this study is more focussed on the %R at 3.2 kPa since cracking is more critical at higher stress level.

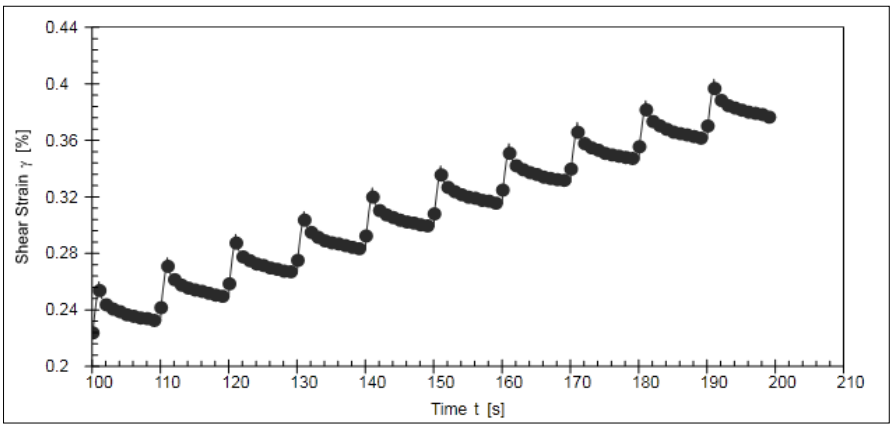

(a) Creep and recovery cycles of SD 4 mastic

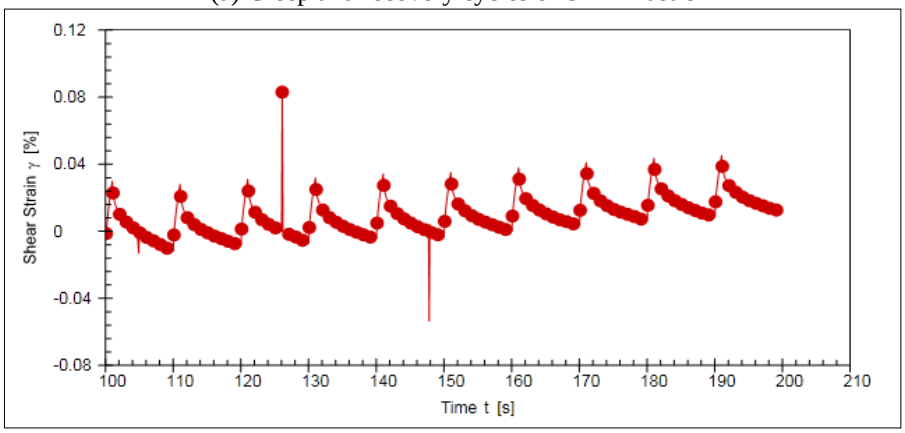

(a) Creep and recovery cycles of GL 8.5 mastic

Figure 6.37 Creep and recovery cycles of SD 4 and GL 8.5 mastics

The %R values of bitumen and mastics are stated in Table 6.11. It was observed that the MSCR test was able to distinguish between the different mastics. Figure 6.37 displayed the 10 cycles of creep and recovery MSCR testing of long-term aged SD 4 mastic. The curves observed are fairly smooth and have no jagged edges, which suggest that the use of MSCR test for determining fatigue resistance is technically feasible without sacrificing data accuracy. However, creep and recovery curves of GP 8.5 and GL 8.5 mastics were found to be distorted and hence these mastics were not taken in investigation. This might be due to the technical inability of the DSR to test excessively stiff mastics.

The %R of mastics was found to be higher than the bitumen. In addition to that the %R recovery was found to increase with the increase in filler content. Similar trend was observed in section 6.5.1.6.2, when testing of %R is done at higher temperatures (46-70°C). The reason behind this behavior is same and can be referred in that section only. Results suggested that the fatigue resistance of mastic increased with the filler content. GL mastics were found to have higher fatigue resistance followed by GP, KS, and, SD mastics. Both results are in contrast with the trend determined by the previous two methods. Some previous studies have suggested that the fatigue resistance determined from different test methods displayed different trends (Monismith et al., 1990; Zhou et al., 2012). In both Superpave fatigue parameter and LAS tests, strain is being maintained throughout the testing period. However the MSCR is stress based testing and strain is being varied during testing. Hence it seemed that the mode of testing also significantly affects the testing results. The mastic having higher %R has given higher ranking. However, there are some cases such as SD 8.5, GP 4, and KS 5.5, in which all mastics have almost similar %R

(70.24, 70.92, and 70.12%). In such cases, the %R at 0.1 kPa is also observed and the mastic having higher %R at 0.1 kPa (SD 8.5) has allotted higher ranking and vice versa. The rankings determined from Superpave fatigue parameter, LAS analysis, and MSCR analysis was compared in Table 6.12. These rankings will further be compared with the fatigue life of the bituminous mixes determined in the subsequent sections of the study.

Table 6.11 Percentage recovery of bitumen and various mastics at 25°C

Type of mastic	%R (0.1 kPa) (%)	%R (3.2 kPa) (%)
Bitumen	62.75	58.83
SD 4	71.06	65.42
SD 5.5	74.27	67.25
SD 7	75.67	68.13
SD 8.5	81.87	70.24
GP 4	77.10	70.92
GP 5.5	86.10	73.68
GP 7	84.22	79.40
GP 8.5	-	-
KS 4	74.83	66.23
KS 5.5	79.84	70.12
KS 7	77.21	68.92
KS 8.5	85.41	74.84
GL 4	78.03	72.75
GL 5.5	82.15	76.23
GL 7	88.24	87.13
GL 8.5	-	-

Table 6.12 Ranking of bitumen and mastics using different methods

Type of mastic	Ranking		
	Fatigue parameter	LAS	MSCR
Bitumen	1	1	15
SD 4	2	3	14
SD 5.5	4	4	12
SD 7	8	8	11
SD 8.5	11	12	7
GP 4	5	6	9
GP 5.5	10	9	5
GP 7	12	13	2
GP 8.5	14	16	-

KS 4	3	2	13
KS 5.5	6	5	8
KS 7	9	10	10
KS 8.5	13	15	4
GL 4	7	7	6
GL 5.5	15	11	3
GL 7	16	14	1
GL 8.5	17	17	-

6.5.6.3 *Long-Term Ageing Resistance*

To investigate the effects of ageing on the mechanical properties of bitumen and mastics, an Ageing Index (AI) was calculated. AI was calculated for bitumen and mastics based on short-term and short plus long-term aged complex shear modulus (G*), measured at 10 rad/s frequency and 25 and 64°C temperatures using Equation 6.11. The testing at 25°C was done with 8 mm parallel plate geometry arrangement having 2 mm gap; while for testing at 64°C, arrangement with 25 mm parallel plate geometry and 1 mm gap is chosen. This parameter is used to determine the rheological implication of ageing in bitumen and mastics. Higher value of AI indicates higher ageing susceptibility and vice versa.

$$AI = \frac{G^*_{LTA}}{G^*_{STA}} \qquad [6.11]$$

Where, G^*_{LTA} is complex shear modulus of mastic subjected to short plus long-term ageing and G^*_{STA} is complex shear modulus of mastic subjected to short-term ageing alone.

Table 6.13 Complex shear modulus of mastics at different temperatures and ageing

Complex shear modulus of bitumen and mastics (kPa)				
Type of conditioning	Short-term aged		Short-term + Long-term aged	
Testing temperature / Type of mastic	25°C	64°C	25°C	64°C
Bitumen	1129	5.76	1738	22.07
SD 4	1562	12.98	2334	38.16
SD 5.5	2971	16.42	3892	39.74

SD 7	4530	19.81	5300	44.17
SD 8.5	8034	31.23	8757	61.52
GP 4	3259	18.93	4399	48.65
GP 5.5	4778	23.52	6211	50.56
GP 7	8002	34.33	9442	66.94
GP 8.5	11672	53.32	12956	100.77
KS 4	2559	15.75	3582	46.93
KS 5.5	3964	19.87	4916	48.48
KS 7	5312	26.00	6746	49.92
KS 8.5	10848	39.98	10956	69.16
GL 4	4356	23.10	5576	51.05
GL 5.5	8991	30.55	10429	60.49
GL 7	11252	45.45	12602	75.01
GL 8.5	13335	62.16	14402	101.70

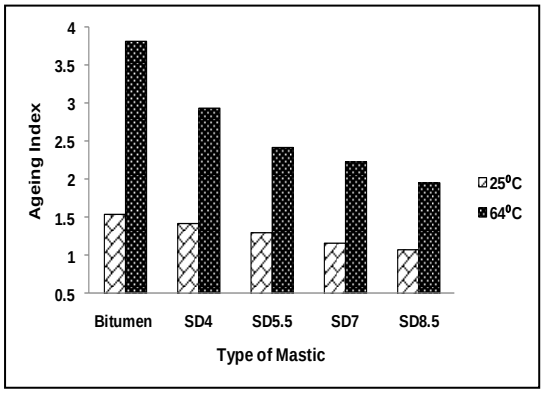

(a) Ageing Index of SD mastics

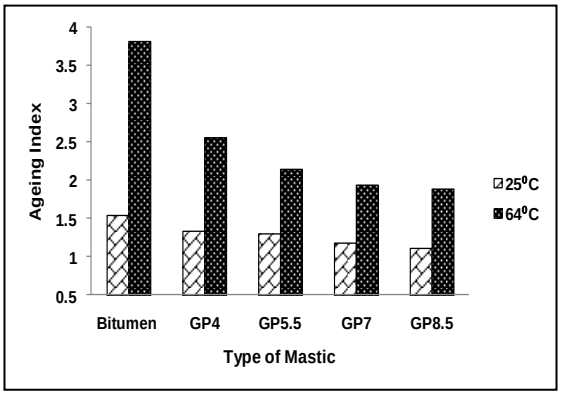

(b) Ageing Index of GP mastics

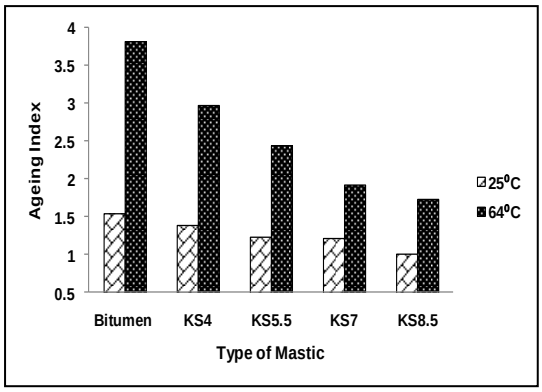

(c) Ageing Index of KS mastics

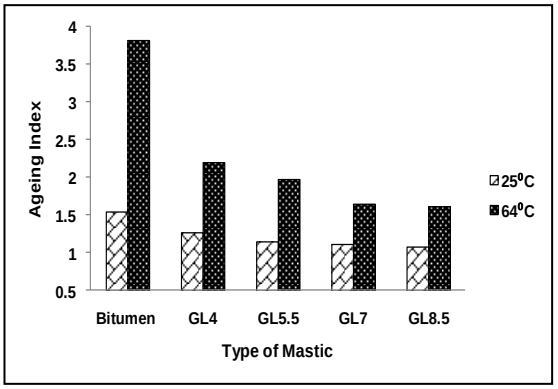

(d) Ageing Index of GL mastics

Figure 6.38 Ageing Index of bitumen and mastics at 25 and 64°C

The G* values of the bitumen and mastics at both temperatures are shown in Table 6.13. It can be clearly seen that ageing tends to increase the G* of both bitumen and mastics. This increase in the stiffening is due to the oxidation of lighter components

of bitumen (saturates and aromatics) to the heavier fractions (resins and asphaltenes) (Fernández-Gómez et al., 2013; Liu et al., 2018). This resulted in the transformation of visco-elasticity of bitumen to elasticity which resulted in the increase of G* values. Hence the AI of bitumen and mastics can't be lower than unity. The AI of bitumen and mastics are shown in Figure 6.38. It can be seen that bitumen exhibited higher age hardening at both temperatures than the mastics and has higher ageing index. In addition to this, the age hardening of the mastics was found to reduce with the increase in filler concentration at both temperatures. According to various literatures discussed in Chapter 2 of this study, the ageing of the mastic not only depends on the physical characteristics of the fillers but also on their molecular interaction with the bitumen. The increase in the filler volume fraction in the mastic with the simultaneous decrease in bitumen volume fraction tends to decelerate the age hardening of the bitumen in the mastic. The presence of the fillers in the mastic imparts impermeability to the oxygen diffusion, which reduces the oxidation of bitumen. As the filler volume fraction increases in the mastic, the oxygen molecules required to take a more tortuous path in the bitumen which inhibits the oxidation of bitumen and hinder the rise in its stiffness (Moraes and Bahia, 2015).

The mastics prepared with GL displayed lowest AI and hence exhibited lower sensitivity to ageing followed by GP, KS, and SD mastics. GL mastic has the highest filler volume fraction and thus prevents the diffusion of the oxygen and maintains the softening of the mastic. Although GP mastics also has the almost similar volume fraction, it displays higher AI than GL mastics. This might be due to the reason that GL consists of hydrated lime which is also a widely recognized to display anti ageing bitumen due to the acid-base reaction between the polar molecules of the bitumen and

the hydrated lime surface (Alfaqawi et al., 2017; Lesueur et al., 2013; Lesueur et al., 2016; Petersen 2009; Petersen et al., 1987). Thus, the additional decrease in the ageing index in GL mastics might be due to addition filler bitumen interaction between hydrated lime and bitumen. It is also interesting to notice that despite having relatively lower filler volume fraction, KS 8.5 mastic displayed lower AI than GP 8.5. This might be due to the alkaline nature of KS which interacts well with the bitumen due to its acidic nature and prevents the oxidation of bitumen (Petersen et al., 1987; Wisneski et al., 1996). The ageing susceptibility of mastics was found to increase with the increase in testing temperatures, and AI at 64°C was always found to be higher than that at 25°C. A recent study (Rochlani et al., 2019) also found the similar trend. Mastics tested at 64°C displayed much higher fluidity than the mastics at 25°C. This might have resulted in relatively free movement of filler in the mastic that may have resulted in higher filler-filler and filler bitumen interaction, which may resulted in the increase in their ageing susceptibility. This aspect need to be explored further in future studies.

6.6 Summary

This chapter analyzed the rheological responses of bitumen and various bituminous mastics in terms of rutting, fatigue, and long-term ageing. The mastics were prepared according to the filler bitumen ratios finalized at the end of the previous chapter. These mastics were aged according to standard protocols and were tested in various combinations of loading frequency and temperatures. The consistency of short-term aged bitumen and mastics were analyzed using softening point test. It was observed that inclusion of filler in the mastics increases its stiffening which consequently increase their softening point. GL and GP mastics displayed highest softening points

followed by KS and conventional SD mastics. Since softening point is an empirical test, which doesn't accounts the influence of the loading frequency and temperature, dynamical mechanical analysis was also conducted using DSR.

The rheological properties of bitumen and mastics were analyzed at intermediate (25°C) and high temperatures (46-70°C) for different frequencies (0.1-100 rad/s). The intention was to conduct the analysis within the linear viscoelastic region, hence the linear viscoelastic (LVE) limit of bitumen and mastics were determined using strain sweep test. The LVE limit for the mastics was found to decrease with the increase in filler content and decrease in temperature. The mastics having higher stiffening (GL and GP) exhibited lower LVE limits and vice versa. Mastics also displayed lower temperature susceptibility than plain bitumen, as they exhibited lower rate of LVE increase with the temperature. The rheological analysis was done at the strains lower than the LVE limit of mastics. The frequency sweep test was conducted at intermediate and high temperatures for a given frequency range (0.1-100 rad/s) to analyze the rheological properties (complex modulus and phase angles) of short-term aged bitumen and mastics. The data was represented in the forms of isothermal curves and black diagrams. The increase in complex modulus and decrease in phase angle was observed with the increase in filler content at each loading frequency. The stiffness of bitumen and mastics was also found to increase with the decrease in temperature and increase in frequency. For all mastics, the rate of increase in complex modulus with frequency was found to increase with the testing temperature. It inferred that the mastics become more susceptible to frequency at higher temperature. It was also observed that at the same temperature, mastics having higher stiffness exhibited lower rate of growth in complex modulus. Hence it can be inferred that the

stiffer mastics are less susceptible to the rate of traffic loading and vice versa. The rate of decrease in phase angle was also found to decrease with increase in the temperature. At the same frequency (10 rad/s), GL mastics displayed highest complex modulus and lowest phase angle followed by GP, KS, and SD. This might be attributed to higher filler volume fraction and angular nature of glass powder in the mastics. All mastics (especially GL and GP mastics) displayed steady growth in complex modulus up to 5.5% filler concentration and then experienced a relatively rapid growth (higher slope) at higher concentration (7 and 8.5%). It was attributed to higher filler bitumen and filler-filler interaction in mastics prepared at higher filler volume. Black diagrams of GL and GP mastics don't exhibit simple smooth curves at higher filler concentration, especially at higher temperature and lower frequency. This confirms that in GL and GP mastics, the filler volume concentration dominates the viscoelastic behaviour of the mastics.

The rutting resistance of short-term aged mastics were compared at higher temperatures using Superpave rutting parameter and MSCR tests. Both tests exhibited more or less similar trends and the rutting resistance was found to increase with increase in filler content and a decrease in temperatures. As expected, the GL mastics displayed highest rutting resistance of GL followed by GP, KS, and SD mastics. Similar trend was also found in terms of elasticity of mastics at different stress levels. Also, barring a few exceptions (GP 8.5, GL7, and GL 8.5), stress sensitivity of the bitumen and mastics was found to increase with the increase in temperature.

The fatigue resistance of long-term aged mastics were determined at 25^{o}C using Superpave fatigue parameter and LAS test. The fatigue behaviour of bitumen and

mastics was also analyzed in terms of percentage elasticity recovery using MSCR test which is a relatively new approach. The fatigue resistance determined by fatigue parameter and LAS test exhibited more or less similar trends. The fatigue resistance of mastics decreased with the increase in filler contents. In general, SD mastics displayed highest fatigue resistance followed by KS, GP, and GL mastics. However, LAS test was found to be more practical since it evaluated the complex behavior of the bitumen mastics at a wide range of loading level. LAS test suggested that fatigue life of bitumen and mastics decreased with the increase in applied strain. MSCR test displayed almost inverse trend than the two former methods and suggested that the inclusion of filler improved the fatigue performance of the mastics. The results obtained by the test methods need further validation with performance analysis of bituminous mixes.

The long-term ageing susceptibility of bitumen and mastics was analyzed at 25 and 64°C by determining their ageing index based on complex modulus values. The ageing susceptibility of the mastics decreased with the increase in filler concentration. The presence of the fillers in the mastic found to imparts impermeability to the oxygen diffusion, which reduces the oxidation of bitumen. The ageing susceptibility of mastics was also found to increase with the increase in testing temperatures, and ageing index at 64°C was always found to be higher than that at 25°C. GL mastics displayed the superior resistance due to higher filler volume fraction and acid base reaction between hydrated lime and bitumen. GP mastics exhibited higher ageing resistance at lower filler concentration than KS mastics. However at higher concentration, KS mastic displayed relatively better ageing resistance than GP, owning to its alkaline nature and better interaction with bitumen.